CHAPTER THREE

SALEN-SUPPORTED COBALT CATALYSTS IN COMBINATION WITH ORGANIC-BASED, IONIC OR LEWIS BASIC COCATALYSTS FOR PROPYLENE OXIDE/CO_2 COPOLYMERIZATION: HIGH ACTIVITY AND SELECTIVITY

Reprinted in part with permission from the

Journal of the American Chemical Society **2005**, *127*, 10869 – 10878.

Journal of Polymer Science, Polymer Chemistry **2006**, *In Press*.

3.1 Introduction

We have shown that (salen)CoX (X = halide or carboxylate) PO/CO_2 copolymerization catalysts are highly selective for PPC formation with excellent control of polymer microstructure (Chapter 2).[1] Notably, catalyst activities for this transformation are inferior to zinc- or chromium-based alternatives.[2-7] It has been presented independently by Inoue, Darensbourg, and Lu that the coupling of porphyrin or salen-type metal catalysts with organic-based, ionic compounds has resulted in improved catalytic activities in a variety of polymerization systems.[6, 8-19] Similar to the catalysts we report, the addition of ammonium-based, ionic cocatalysts (*n*-Bu_4NY; Y = Cl, Br, I) to (*R,R*)-(salen-**1**)CoX (X = OAc (**2.1**), O_2CCCl_3, O_2CCF_3, Cl (**2.4**), OTs; Ts = *p*-toluenesulfonyl) in the presence of PO and CO_2, shows reaction rates that are sensitive to the anionic components (X and Y) for the generation of PC.[20] Although it was originally thought that ammonium-based, ionic cocatalysts limited the (*R,R*)-(salen-**1**)CoX catalyzed reaction of PO and CO_2 to the production of PC, PPC was recently achieved through the careful choice of the complex and cocatalyst.[12] Specifically, (*R,R*)-(salen-**1**)CoOAr (Ar = 4-nitrophenyl, 2,4-dinitrophenyl, or 2,4,6-trinitrophenyl) derivatives with [*n*-Bu_4N]Y (Y = Cl, OAc) cocatalysts were described by Lu and coworkers to afford PPC with exceptional rates and selectivity while using low CO_2 pressures.[21]

Lewis basic cocatalysts have likewise been added to porphyrin or salen-type catalysts for improvement of epoxide/CO_2 polymerization rates.[2, 4-7, 13-16, 21-24] Recently, Darensbourg and coworkers have shown that the steric and electronic nature of the Lewis base used has a large influence on catalyst activity using (salen)CrN_3 catalysts for CHO/CO_2 copolymerization, attributable to the ability of the cocatalyst to bind to the active chromium center and react with CO_2.[13] Similar to our (salen)CoX catalysts, Nguyen has shown that addition of (*R*)-(+)-4-

(dimethylamino)pyridinyl(pentaphenylcyclopentadienyl)iron to (*R,R*)-(salen-**5**)$CoNO_3$ results in a large catalyst rate enhancement at moderate CO_2 pressures (350 psig).[22] Lu has also combined salen-supported cobalt catalysts with Lewis bases, and has compared the properties of the Lewis base used to the resultant cocatalyst performance; alike the studies described by Darensbourg for chromium-based systems.[21]

Since our discovery of the active (*R,R*)-(salen-**1**)CoX (X = halide or carboxylate) catalysts,[1] we have furthered catalyst optimization, which has led to the use of both organic-based, ionic cocatalysts similar to those reported by Inoue, Darensbourg, and Lu,[6, 8-19] as well as Lewis basic cocatalysts similar to those reported by Inoue, Darensbourg, Rieger, Lu, and Nguyen.[2, 4-7, 13-16, 21-24] We explore the effects of cocatalysts on catalyst activity, product selectivity, stereo-, and regioselectivity while employing a series of different catalyst ligands and reaction conditions. Following optimization, we observe a polymerization rate enhancement up to an order of magnitude greater that that of the (salen)CoX catalysts alone. Additionally, we describe the diverse PPC stereo- and regiochemistries that result from variation of the catalyst and PO stereochemistry and reaction conditions employed, and suggest mechanistic possibilities based on analysis of PPC end-groups and microstructure. Notably, these optimized systems demonstrate unprecedented reaction rates and selectivity for highly regioregular PPC.

3.2 Addition of cocatalysts for improved activity and selectivity

3.2.1 Addition of Cocatalyst [PPN]Cl

With the goal of increasing PO/CO_2 copolymerization activities using catalysts (salen)CoX, we initially added bis(triphenylphosphine)iminium chloride ([PPN]Cl), a commercially available, readily dried (hydrophobic) organic-based, ionic compound[25] with a bulky cation and a nucleophilic anion (Figure 3.1). We then screened our

catalyst library with [PPN]Cl for *rac*-PO/CO_2 copolymerization activity at low CO_2 pressures (200 psi) to look for an increase in reaction rates. Notably, we observed a remarkable improvement in catalyst activities, as well as increased stereo- and regioselectivities when [PPN]Cl was combined with any of the (*R,R*)-(salen-**1**)CoX complexes (Table 3.1).

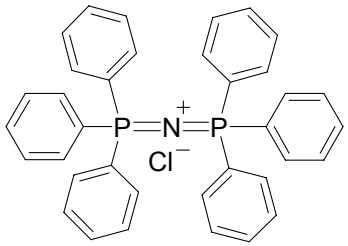

Figure 3.1. [PPN]Cl cocatalyst.

Table 3.1. Effect of initiating group with cocatalyst [PPN]Cl: (*R,R*)-(salen-**1**)CoX (X = OAc (**2.1**), $OBzF_5$ (**2.3**), Cl (**2.4**), Br (**2.5**)) catalyzed *rac*-PO/CO_2 copolymerization.[a]

Entry	Complex	PPC Yield[b] (%)	TOF[c] (h^{-1})	Selectivity (PPC:PC)	M_n[d] (kg/mol)	M_w/M_n[d]	Head-to-Tail Linkages[e] (%)
1	**2.1**	10	110	86:14	7.9	1.15	93
2	**2.3**	49	490	>99:1	43.0	1.10	93
3	**2.4**	43	430	>99:1	35.4	1.09	95
4	**2.5**	41	410	89:11	33.2	1.09	95

[a] Copolymerizations run neat with [*rac*-PO]:[Co]:[[PPN]Cl] = 2000:1:1 at 22 °C with 200 psi of CO_2 for 2 h. All product PPC contains ≥ 98% carbonate linkages as determined by ^{1}H NMR spectroscopy ($CDCl_3$, 300 MHz). [b] Based on isolated PPC yield. [c] Turnover frequency for PPC = (mol PO/(mol Co · h)). [d] Determined by GPC calibrated with polystyrene standards in THF at 40 °C. [e] Determined by quantitative $^{13}C\{^1H\}$ NMR spectroscopy ($CDCl_3$, 125 MHz, d_1 = 10s).

By itself, [PPN]Cl demonstrated no activity for the copolymerization of *rac*-PO and CO_2, whereas in combination with complex (*R,R*)-(salen-**1**)CoOBzF_5 (**2.3**), PPC was generated with an activity of 520 turnovers per hour (Table 3.1, entry 2). The product PPC is nearly completely alternating, with 93% HT connectivity with a high M_n and a narrow MWD. Complexes **2.4** and (*R,R*)-(salen-**1**)CoBr (**2.5**) with [PPN]Cl also exhibit outstanding catalytic activity; however, selectivity for polymer is reduced with the latter (entries 3 and 4). The copolymerization catalyzed by **2.1** with [PPN]Cl is significantly slower than that catalyzed by all other catalyst/[PPN]Cl combinations, and the selectivity for generating PPC over PC is also somewhat compromised (entry 1).

3.2.2 Reaction time and solvent

Using the most active **2.3**/[PPN]Cl catalyst system, PPC is generated in 32% yield after 1 h and in 52% yield after 2 h, corresponding to catalyst TOFs of 620 h^{-1} and 520 h^{-1} respectively (Table 3.2, entries 1 and 2). In each case, only trace PC byproduct is observed. At extended reaction times, however, the overall selectivity for polymer is decreased notably (entry 3). We observed that at approximately 50% conversion, the polymerization solidifies, and the byproduct PC is formed instead of polymer. In an effort to maximize polymer yield, it is crucial to quench the copolymerization upon reaching approximately 50% conversion. In order to achieve PPC at higher % conversions, the addition of solvent is required.

Table 3.2. Effect of reaction time: (*R,R*)-(salen-**1**)CoOBzF$_5$ (**2.3**)/[PPN]Cl catalyzed *rac*-PO/CO_2 copolymerization.[a]

Entry	Time (h)	PPC Yield[b] (%)	Selectivity (PPC:PC)	M_n[c] (kg/mol)	M_w/M_n[c]
1	1	31	99:1	26.8	1.13
2	2	52	>99:1	43.0	1.10
3	6	59	56:46	41.4	1.36

[a] Copolymerizations run neat with [*rac*-PO]:[**2.3**]:[[PPN]Cl] = 2000:1:1 at 22 °C with 200 psi of CO_2. All product PPC contains ≥ 98% carbonate linkages as determined by ^{1}H NMR spectroscopy ($CDCl_3$, 300 MHz). [b] Based on isolated PPC yield. [c] Determined by GPC calibrated with polystyrene standards in THF at 40 °C.

The maximum **2.3**/[PPN]Cl catalyst activity is observed when carrying out the copolymerization in neat *rac*-PO (Table 3.3, entry 1) whereas the addition of solvent to the copolymerization slows down the reaction. Generally, non-protic, non-halogenated solvents are beneficial for achieving high PPC conversion. After 4 h, the **2.3**/[PPN]Cl catalyzed *rac*-PO/CO_2 copolymerization in an equivolume mixture of *rac*-PO and 1,2-dimethoxyethane (DME) affords 61% conversion to PPC (entry 2). Under the same reaction conditions, increasing the reaction time to 6 h yields 75% PPC with only 2% PC byproduct (entry 3). In this case, the % HT connectivity of the PPC is 92%, which is similar to that observed when no solvent is used. Although the polymerization mixture does not solidify after 6 h in DME, prolonging the *rac*-PO/CO_2 copolymerization time does not improve polymer yield (entry 4). Increasing the amount of DME such that [PO]:[DME] = 1:2 further slows down the copolymerization, where only 55% conversion to PPC is achieved after 6 h (entry 5). At extended reaction times (24 h) PPC is obtained in 81% yield, which is the highest conversion we obtain for this system.

The addition of DME to the **2.3**/[PPN]Cl catalyzed *rac*-PO/CO_2 copolymerization yields PPC with an observed M_n that is lower than the calculated theoretical value. Interestingly, changing the solvent to PC or toluene likewise yields PPC with low M_n values (entries 7 and 8). Although chain transfer to trace water introduced by the solvent is possible, we suspect that under the diluted conditions, the propagating PPC can backbite onto the carbonyl near the chain end, resulting in the formation of cyclic polymer. Furthermore, the anion that is liberated from the end of the polymer chain can reinitiate leading to additional PPC chains (Scheme 3.1).

Table 3.3. Effect of solvent on (*R,R*)-(salen-**1**)CoOBzF_5 (**2.3**)/[PPN]Cl catalyzed *rac*-PO/CO_2 copolymerization.[a]

Entry	Solvent	[PO]: [Solvent]	Time (h)	PPC Yield (%)[b]	TOF (h^{-1})[c]	Selectivity PPC:PC	M_n[d] (kg/mol)	M_w/M_n[d]
1	none	NA	0.5	30	600	99:1	9.8	1.18
2	DME	1:1	4.0	61	150	98:2	14.4	1.18
3[e]	DME	1:1	6.0	75	130	98:2	16.2	1.19
4	DME	1:1	8.0	71	89	98:2	26.8	1.13
5	DME	1:2	6.0	55	92	96:4	19.7	1.39
6	DME	1:2	24.0	81	34	92:8	12.2	1.19
7	PC	1:1	6.0	56	93	NA	10.5	1.19
8	Toluene	1:1	6.0	71	120	99:1	15.6	1.21

[a] Copolymerizations run neat with [*rac*-PO]:[**2.3**]:[[PPN]Cl] = 1000:1:1 at 22 °C with 100 psi of CO_2. All product PPC contains ≥ 98% carbonate linkages as determined by ^{1}H NMR spectroscopy ($CDCl_3$, 300 MHz). [b] Based on isolated PPC yield. [c] Turnover frequency for PPC = (mol PO/(mol Co · h)). [d] Determined by GPC calibrated with polystyrene standards in THF at 40 °C. [e] 92% HT connectivity as determined by quantitative $^{13}C\{^1H\}$ NMR spectroscopy ($CDCl_3$, 125 MHz, d_1 = 10s).

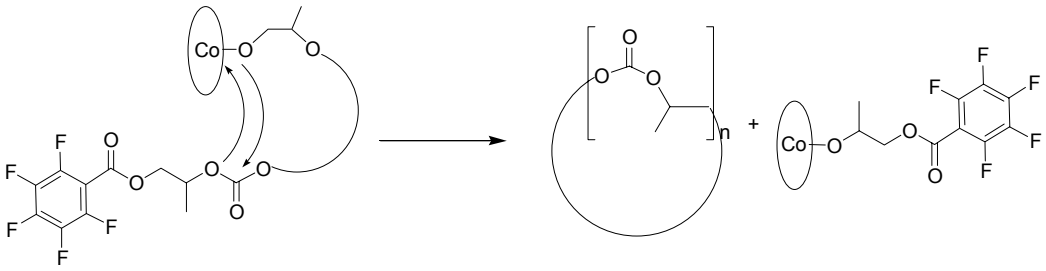

Scheme 3.1. A PPC backbiting mechanism leading to low M_n cyclic PPC with an overall MWD broadening.

3.2.3 CO_2 pressure

In related systems, the coupling of salen-type cobalt catalysts with organic-based, ionic or Lewis basic cocatalysts for PO/CO_2 copolymerization is most effective at low CO_2 pressures.[12, 22] Furthermore, use of low CO_2 pressures for this transformation is attractive, as milder conditions are more amenable for reaction scale up. Although we have shown that the (salen)CoX catalysts are most active for PO/CO_2 copolymerization at high CO_2 pressures (800 psi) (Chapter 2), we observed that low CO_2 pressures are optimal for the **2.3**/[PPN]Cl system, similar to the results presented by Nguyen and Lu.[12, 21, 22]

The *rac*-PO/CO_2 copolymerization using the **2.3**/[PPN]Cl catalyst system at a variety of CO_2 pressures is depicted in Figure 3.2. With a [PO]:[**2.3**]:[[PPN]Cl] loading of 1000:1:1 the copolymerization proceeds at a comparable rate whether 100 or 200 psi of CO_2 is applied. Use of higher or lower CO_2 pressures, however, is detrimental to catalyst activity. We suspect that at pressures below 100 psi the concentration of CO_2 in the solution becomes rate limiting, leading to a decrease in catalyst activity with decreasing pressure. Notably PPC is generated when using only 10 psi of CO_2 with a TOF of 160 h^{-1} with only 15% of PC byproduct formed. In this case, it is necessary to have a constant CO_2 feed as the CO_2 is consumed and

incorporated into the propagating polymer. At high CO_2 pressures (> 200 psi) the reaction rate likewise slows down, which we attribute to the dilution of the solution with CO_2, similar to the results we observed when a solvent is applied. In summary, CO_2 pressures between 100 – 200 psi are ideal for the generation of PPC in minimal time; however, lower pressures can be applied at the cost of overall catalyst activity.

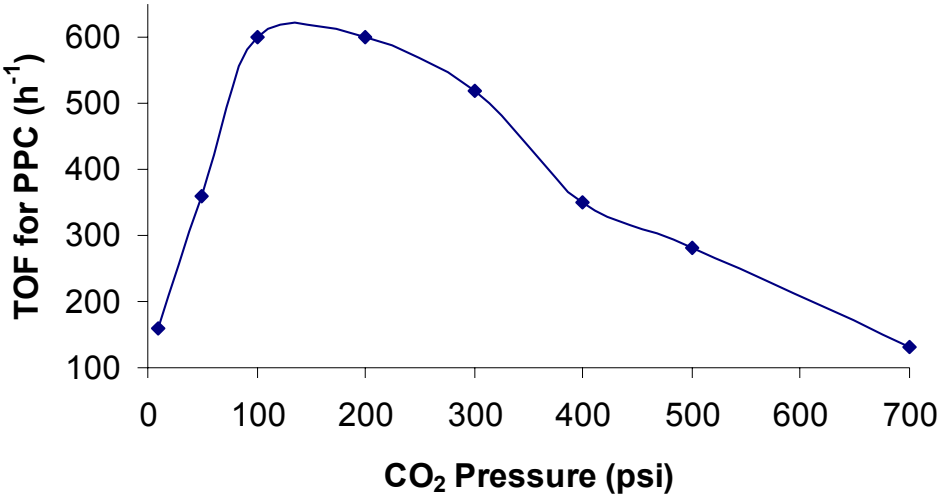

Figure 3.2. Effect of CO_2 pressure: **2.3**/[PPN]Cl catalyzed *rac*-PO/CO_2 copolymerization. Polymerizations run neat at 22 °C with [*rac*-PO]:[**2.3**]:[[PPN]Cl] = 1000:1:1. Reactions run to < 40% PPC conversion.

3.2.4 Temperature

We have previously described that (salen)CoX catalysts have the highest PO/CO_2 copolymerization activities at 22 °C,[1] whereas increasing the temperature leads to catalyst decomposition. As the addition of [PPN]Cl cocatalyst to **2.3** effects numerous changes in catalyst performance, we proceeded to independently study these systems at a series of reaction temperatures. The effect of temperature on the **2.3**/[PPN]Cl catalyzed *rac*-PO/CO_2 copolymerization is collected in Table 3.4. After 1

Table 3.4. Effect of temperature on (*R,R*)-(salen-**1**)CoOBzF_5 (**2.3**)/[PPN]Cl catalyzed *rac*-PO/CO_2 copolymerization.[a]

Entry	Solvent	[*rac*-PO]: [**2.3**]:[[PPN]Cl]	T (°C)	Time (h)	PPC Yield[b] (%)	TOF[c] (h^{-1})	Selectivity PPC:PC	M_n[d]	M_w/M_n[d]	Head-to-Tail Linkages[e] (%)
1	neat	2000:1:1	60	0.5	16	640	57:43	26.5	1.35	79
2	neat	2000:1:1	45	0.5	15	600	52:48	24.1	1.35	85
3[f]	DME	2000:1:1	45	2.0	29	290	91:9	26.4	1.12	84
4	neat	2000:1:1	22	1.0	30	600	98:2	34.0	1.08	96
5	neat	2000:1:1	0	6.0	26	87	>99:1	19.7	1.19	97
6	neat	1000:1:1	-20[g]	10.0	19	19	>99:1	10.5	1.17	98
7	neat	1000:1:1	-20 → 20[g,h]	3.0	39	130	>99:1	19.8	1.19	96
8	neat	500:1:1	-40[g]	8.0	<1	NA	NA	NA	NA	NA

[a] Entries 1 – 4 run with 100 psi CO_2, entries 5 – 8 run with 80 psi of CO_2. All product PPC contains ≥ 98% carbonate linkages as determined by ^{1}H NMR spectroscopy ($CDCl_3$, 300 MHz). [b] Based on isolated PPC yield. [c] Turnover frequency for PPC = (mol PO/(mol Co · h)). [d] Determined by GPC calibrated with polystyrene standards in THF at 40 °C. [e] Determined by quantitative $^{13}C\{^1H\}$ NMR spectroscopy ($CDCl_3$, 125 MHz, d_1 =10s). [f] [PO]:[DME] = 1:1. [g] +/- 8 °C. [h] Warmed up from -20 °C to 22 °C over 3 h.

h at 22 °C ([PO]:[**2.3**]:[[PPN]Cl] = 2000:1:1), PPC is generated with a TOF of 600 h^{-1} with a selectivity for PPC over PC of 99:1 (entry 4). Increasing the temperature to 45 °C, however, results in a decrease in PPC yield, with the generation of 48% PC byproduct (entry 2). Additionally, the MWD of the PPC generated in this case was broadened, and the PPC had only 85% HT connectivity. Although increasing the temperature to 60 °C had comparable selectivity for PPC over PC as in the case of 45 °C, the PPC HT connectivity was decreased from 85% to 79% (entry 1). The formation of PC byproduct at 45 °C can be reduced when DME is used, however catalyst activity is still inferior to that of the neat *rac*-PO/CO_2 copolymerization at 22 °C, and the PPC formed is less regioregular (entry 3).

As increasing the reaction temperature was detrimental to catalyst regioselectivity, we suspected that this trend could be reversed through lowering reaction temperatures below 22 °C. This was indeed the case, where the **2.3**/[PPN]Cl catalyzed *rac*-PO/CO_2 copolymerization carried out at -20 °C yields PPC that is near perfectly regioregular and that is highly isoenriched (Table 3.4, entry 6 and Figure 3.3). In this case the [*rr*], [*rm*], and [*mr*] triad resonances are approximately equal in magnitude and are each close to $1/6^{th}$ that of the [*mm*] shift. This [*rr*]:[*rm*]:[*mr*]:[*mm*] ratio of 1:1:1:6 supports that the polymerization proceeds via a enantiomorphic-site control mechanism (Schemes 2.3 and 3.2). Decomposition of the PPC to PC while maintaining all stereocenters yields a (*S*)-PC:(*R*)-PC of 89:11 (selectivity factor, α = 0.89) as determined by GC (Table 3.5 entry 6). Using equation 3.1 we calculate a k_{rel} for (*S*)- over (*R*)-PO of 9.7. Notably, this preference for (*S*)- over (*R*)-PO is nearly twice the highest value reported in related systems.[1, 12, 22] Finally, using the enantiomorphic-site expressions in the Bovey formalism for PPC triad sequences, we calculate [*mm*] = 0.70, [*rr*] = 0.10, [*rm*] = 0.10, and [*mr*] = 0.10 which is consistent with what we observe in the deconvoluted $^{13}C\{^{1}H\}$ NMR spectrum.

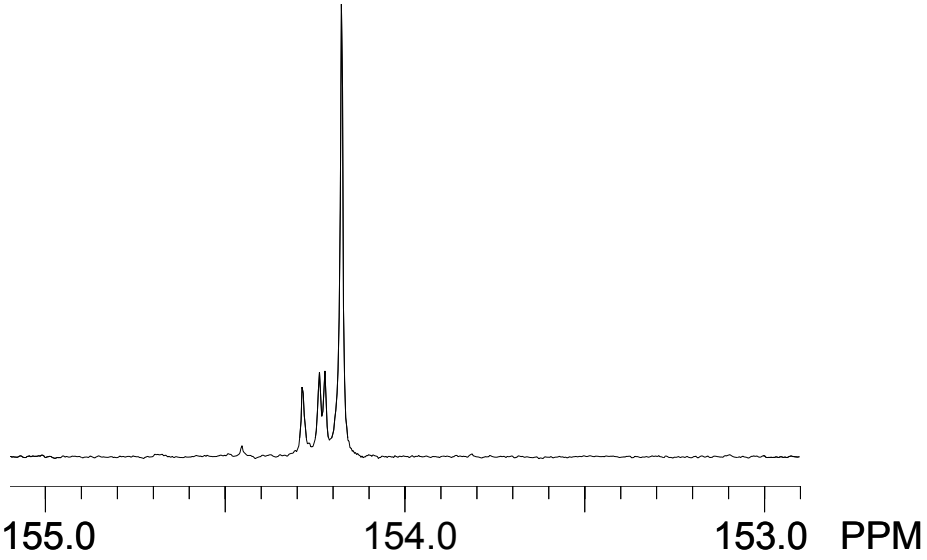

Figure 3.3. Carbonyl region of the quantitative $^{13}C\{^1H\}$ NMR spectrum ($CDCl_3$, 125 MHz, d_1 = 10s) of iso-enriched PPC as generated using catalyst system (*R,R*)-(salen-**1**)$CoOBzF_5$ (**2.3**)/[PPN]Cl and *rac*-PO/CO_2 at -20 °C.

Table 3.5. Selectivity for (*S*)- over (*R*)-PO: (*R,R*)-(salen-**1**)$CoOBzF_5$ (**2.3**)/[PPN]Cl catalyzed *rac*-PO/CO_2 copolymerization at various temperatures (as reported in Table 3.4).[a]

Table 3.4 Entry	%*ee* [(*S*)-stereocenters][b]	α[c]	k_{rel}[d]	[*mm*] calc.(obs.)[e]	[*mr*] + [*rm*] calc. (obs.)[e]	[*rr*] calc. (obs.)[e]
4	60	0.80	5.1	0.52 (0.51)	0.32 (0.32)	0.16 (0.17)
5	68	0.84	6.6	0.60 (0.58)	0.27 (0.27)	0.13 (0.15)
6	78	0.89	9.7	0.70 (0.64)	0.20 (0.24)	0.10 (0.12)
7	64	0.82	6.7	0.55 (0.51)	0.30 (0.32)	0.15 (0.17)

[a] PPC obtained according to the conditions detailed in Table 3.4. [b] Determined by decomposition of PPC to PC while maintaining all stereocenters followed by GC analysis of PC formed. [c] Enantioface selectivity parameter for (*S*)-stereocenter of the enantiomorphic site. [d] Relative rate constant for enchainment of (*S*)- over (*R*)-PO. [e] % HT tetrads as calculated from the enantiomorphic site expressions in the Bovey formalism and % HT tetrads as approximated using deconvolution of quantitative $^{13}C\{^1H\}$ NMR spectroscopy ($CDCl_3$, 125 MHz, d_1 = 10s).

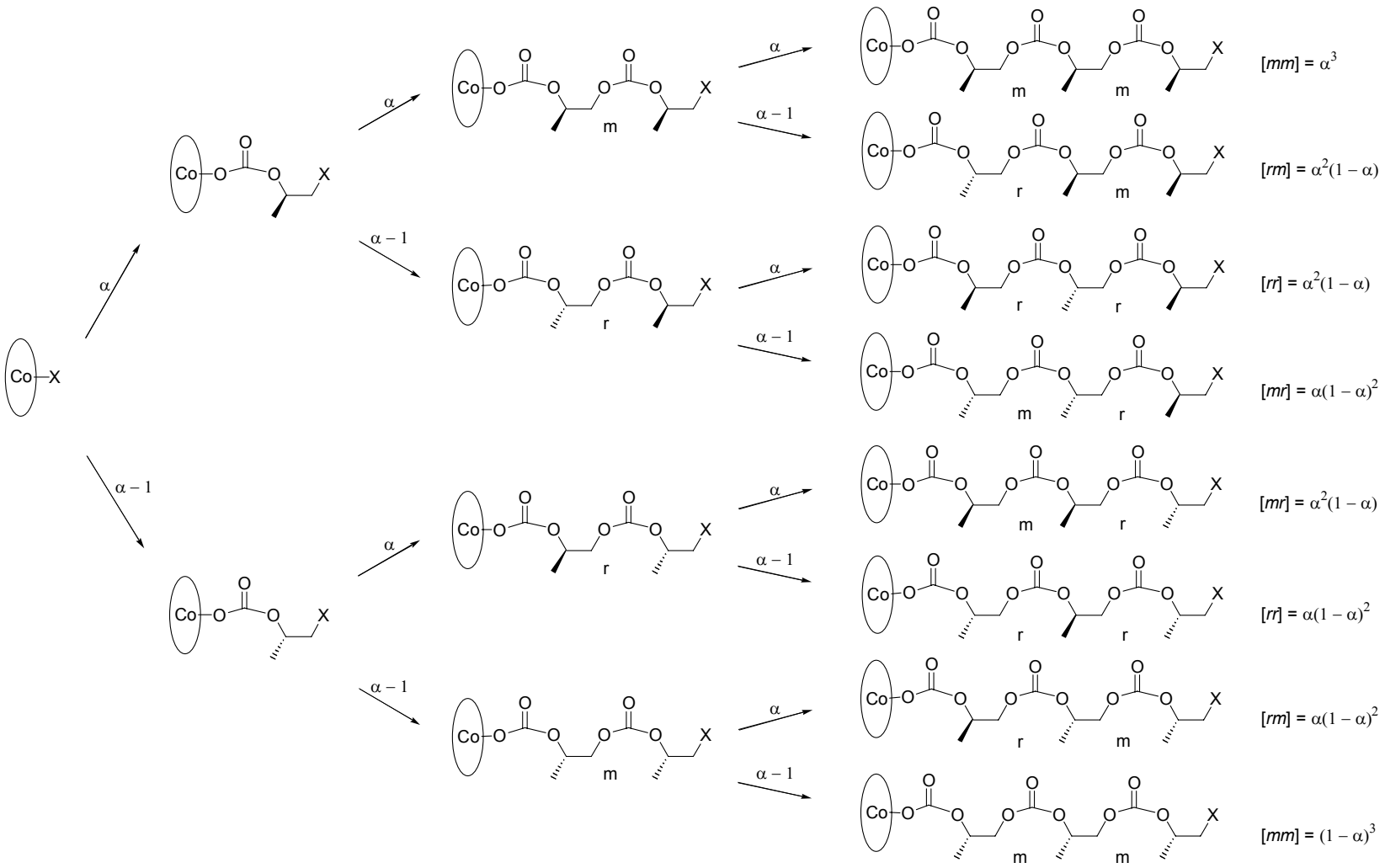

Scheme 3.2. The enantiomorphic-site expressions in the Bovey formalism (α is the enantioface selectivity of the enantiomorphic-site) for PPC triad sequences: $\sum[mm] = \alpha^3 + (1- \alpha)^3$; $\sum[mr] = \sum[rm] = \sum[rr] = \alpha^2(1 - \alpha) + \alpha(1 - \alpha)^2$.

(Eq 3.1.) $$k_{rel} = \ln[(1\text{-}c(1 + ee))]/\ln[(1\text{-}c(1 - ee))]$$

c = conversion, *ee* = enantiomeric excess of product

The **2.3**/[PPN]Cl catalyzed *rac*-PO/CO_2 copolymerization was also carried out at -20 °C and then slowly warmed to 22 °C over the course of 3 h. Not surprisingly, the PPC generated is less stereo- and regioregular compared to the PPC synthesized at a constant -20 °C (Table 3.4 and 3.5, entry 7). This suggests that regio- and stereo-errors are not limited to initiation, and that the selectivity for (*S*)- over (*R*)-PO is highly influenced by the reaction temperature. Furthermore, when the copolymerization is carried out at 0 °C (Table 3.4 and 3.5 entry 5) or 22 °C (Table 3.4 and 3.5, entry 4), we calculate decreased k_{rel} values of 6.6 and 5.1, respectively. Although the **2.3**/[PPN]Cl catalyst system is highly selective at -20 °C, the overall reaction rate slows with decreasing temperature. When the *rac*-PO/CO_2 copolymerization is carried out at -40 °C, only trace PPC is formed after 8 h, despite high catalyst loadings (Table 3.4 entry 8).

3.3 PPC end-group and M_n analysis

3.3.1 PPC end-group analysis

In general, the M_n values of the polymers obtained from the organic-based, ion-assisted copolymerizations in neat *rac*-PO are reproducible and approach 50 kg/mol, yet they are equal to approximately half of the theoretical values based on conversion. We suspect that initiation is not limited to the original initiating group/axial ligand of the cobalt catalyst but also involves the anion from the $[PPN]^+$ cocatalyst. To demonstrate this possibility, PPC was prepared with four different catalyst/cocatalyst combinations: **2.4**/[PPN]Cl, **2.3**/[PPN]Cl, **2.4**/bis(triphenylphosphine)iminium pentafluorobenzoate ([PPN][$OBzF_5$] or **3.1**), and **2.3**/bis(triphenylphosphine)iminium *p*-trifluoromethylbenzoate (**3.2**) (Scheme 3.3). For the later three systems, the isolated polymer showed UV activity by the gel permeation chromatography (GPC) UV detector, whereas the PPC generated by **2.4**/[PPN]Cl did not (Figure 3.4). Furthermore, the ^{19}F NMR spectrum of the PPC generated by either **2.3**/[PPN]Cl or **2.4**/**3.1** revealed that $OBzF_5$ end groups were present. Each spectrum exhibited ^{19}F resonances at δ –138 (m), –149 (m), –161 (m) ppm, consistent with a $OBzF_5$ moiety on the PPC. Finally, the ^{19}F NMR spectrum of the PPC generated by **2.3**/**3.2** revealed that both $OBzF_5$ and *p*-trifluoromethylbezoate end groups were present with ^{19}F resonances at δ -64 (s), –138 (m), –149 (m), –161 (m) ppm and ^1H NMR resonances at δ 7.69 (m), and 8.13 (m), consistent with both a $OBzF_5$ and *p*-trifluoromethylbenzoate moiety on the PPC. These data suggest that initiation occurs from both the catalyst axial ligand as well as from the anion of the cocatalyst. Given that the MWDs of the product polymers remain narrow, we hypothesize that the number of propagating PPC chains is equal to the total number of nucleophiles/initiators present.

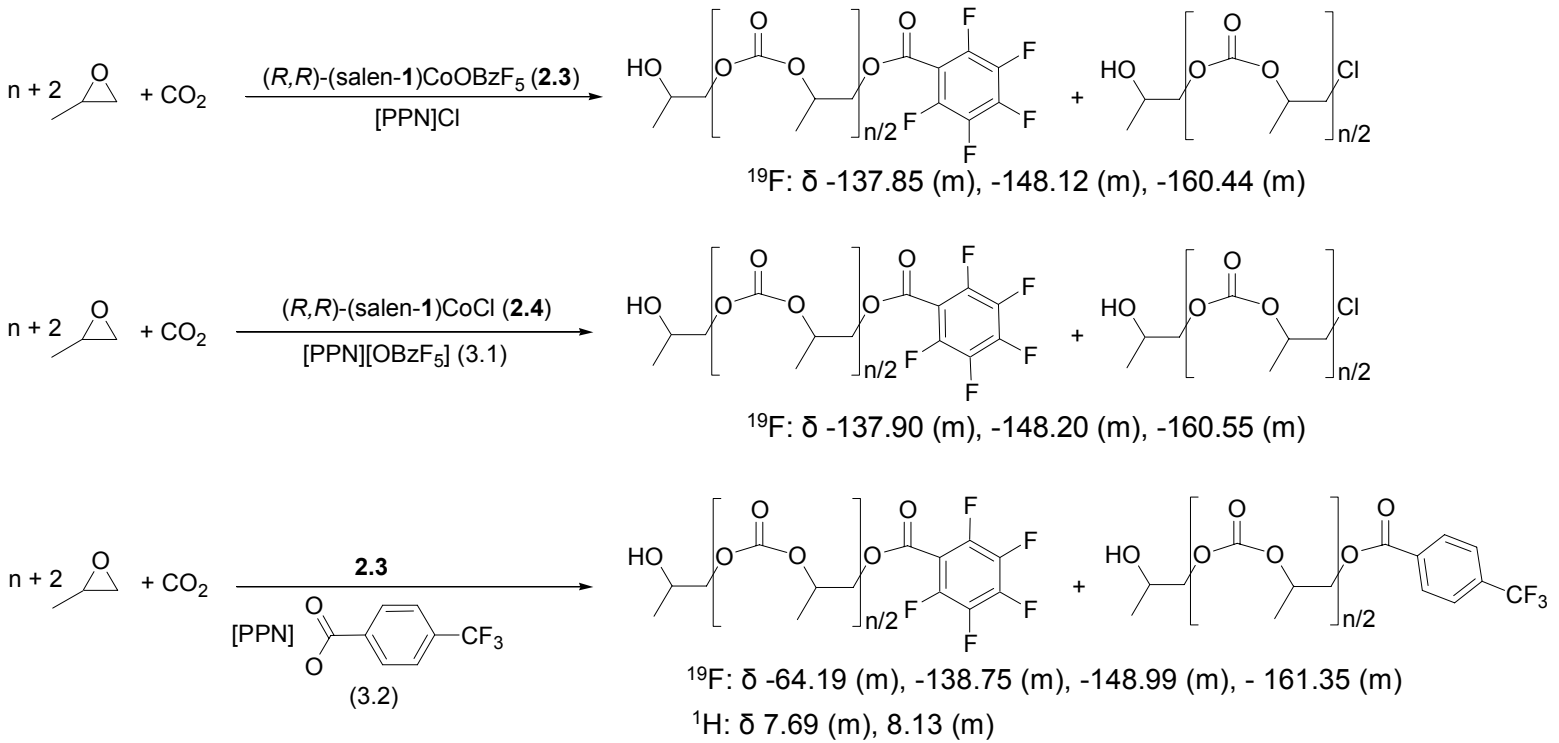

Scheme 3.3. Both the catalyst axial ligand and the cocatalyst anion can be found as endgroups on the PPC generated. ^{19}F NMR ($CDCl_3$, 470 MHz, ref C_6F_6 -162.9 ppm), ^{1}H NMR ($CDCl_3$, 500 MHz).

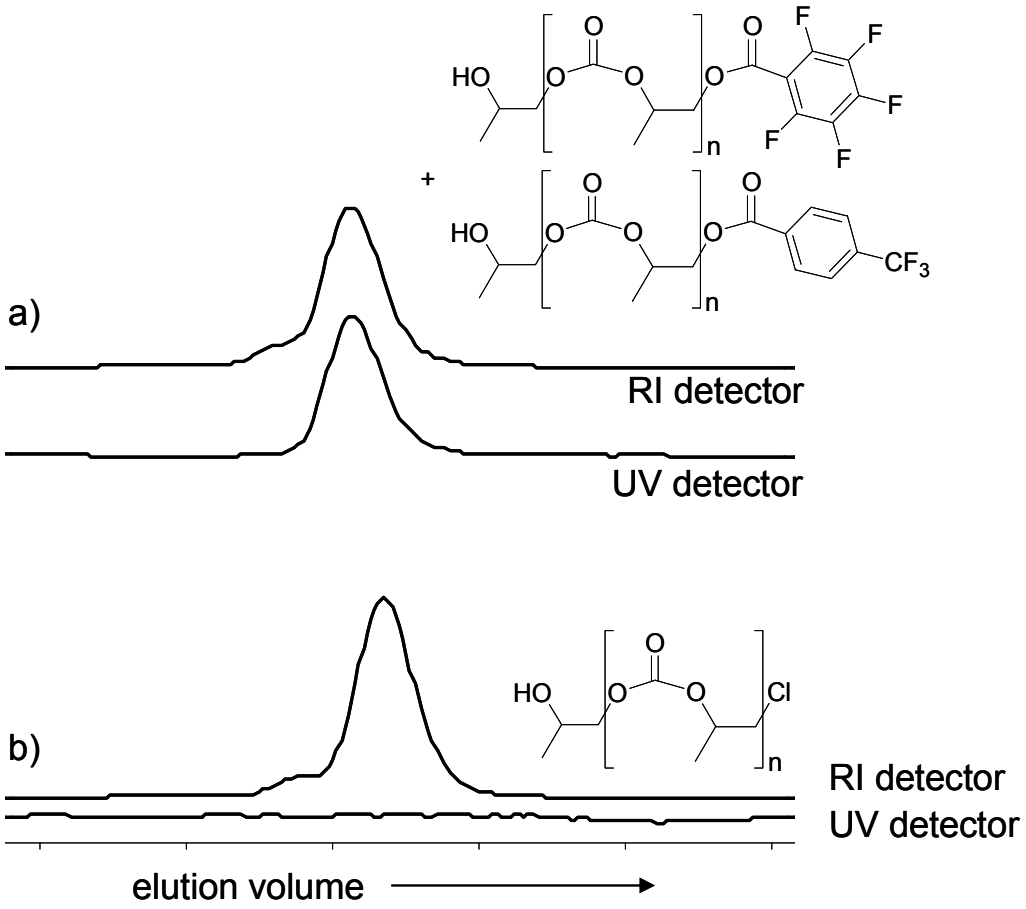

Figure 3.4. GPC trace of PPC with a) UV-active and b) UV-silent end-groups.

3.3.2 Cocatalyst loading

To further support our hypothesis that both the catalyst and anion from the cocatalyst are capable of initiation, we proceeded to run the **2.3** catalyzed PO/CO_2 copolymerization using different equivalents of [PPN]Cl. Figure 3.5 depicts the relationship between the catalyst activity and the relative ratios of the experimental M_ns to the corresponding theoretical M_n values to the amount of [PPN]Cl applied. Although 0.5 equivalents of [PPN]Cl is sufficient to generate PPC using catalyst **2.3** at a [Co]:[PO] loading = 2000:1, catalyst activity is close to half that of when 1

equivalent of [PPN]Cl is used. Interestingly, the relative ratios of the experimental M_ns to the corresponding theoretical M_n values in the two cases reduces from 0.63 to 0.56 when 1.0 and 0.5 equivalents of [PPN]Cl are used, respectively. When 2 equivalents of [PPN]Cl is applied, the experimental/theoretical M_n reduces to 0.25 and catalyst activity increases slightly. Finally, when 5 equivalents of [PPN]Cl is used, the experimental/theoretical M_n reduces is only 0.10 and catalyst activity drops dramatically. Overall, although increasing the amount of [PPN]Cl up to 2 equivalents increases catalyst activity, the addition of this cocatalyst is detrimental to PPC molecular weight.

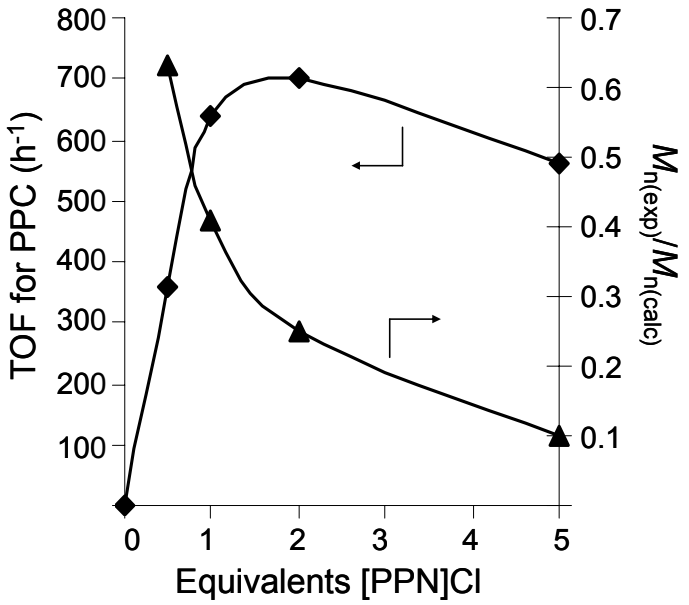

Figure 3.5. The amount of [PPN]Cl cocatalyst influences catalyst activity and the M_n value of the PPC formed. Polymerizations run neat at 22 °C with [*rac*-PO]:[**2.3**] = 2000:1 with 100 psi of CO_2. Reactions run to < 40% PPC conversion.

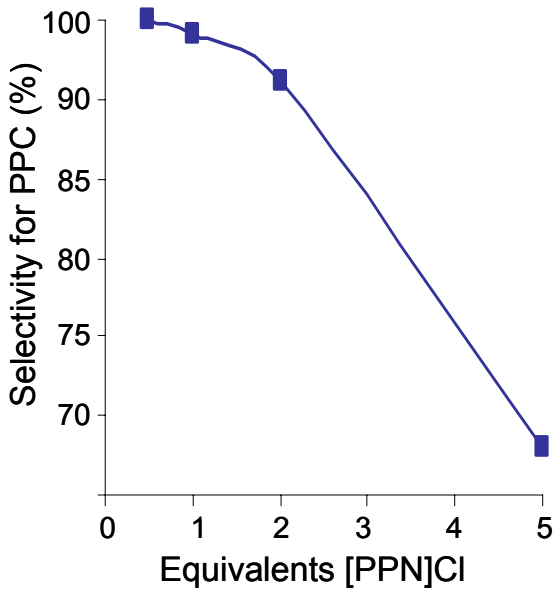

Figure 3.6. The amount of [PPN]Cl added influences the selectivity for PPC over PC. Polymerizations run neat at 22 °C with [*rac*-PO]:[**2.3**] = 2000:1 with 100 psi of CO_2. Reactions run to < 40% PPC conversion.

The selectivity for PPC over PC is also influenced by the amount of [PPN]Cl present in the copolymerization. Figure 3.6 shows the relationship between the equivalents of [PPN]Cl used and the resultant selectivity for PPC over PC. When 0.5 or 1 equivalent of [PPN]Cl is used, the catalyst system is highly selective for PPC, with only up to 2% PC observed in the later case. When more [PPN]Cl is added, however, selectivity for PPC decreases sharply, where the catalyst system is only 73% selective for PPC when 5 equivalents of [PPN]Cl is applied. When 50 equivalents of [PPN]Cl is used, the relative PC to PPC formed is greater than 99:1. As we do not observe PC or PPC formation when [PPN]Cl is used without catalyst **2.3** under comparable reaction conditions, we suspect that the excess [PPN]Cl behaves as a

chain-transfer agent, displacing PC rather than propagating polymer. In summary, increasing the amount of [PPN]Cl cocatalyst in the **2.3** catalyzed *rac*-PO/CO_2 copolymerization results in decreased PPC molecular weight, which is consistent with our hypothesis that both the catalyst axial ligand and the anion from the $[PPN]^+$-based cocatalyst is capable of initiation. Furthermore, as we do not observe a linear dependence between experimental M_n/theoretical M_n values and the amount of [PPN]Cl added, we suspect that some of the anions/nucleophiles present facilitate the generation of PC.

3.3.3 Immortal behavior

We have shown that the inclusion of water into the (*R,R*)-(salen-**1**)CoX (X = OAc or I) catalyzed PO/CO_2 copolymerization results in a broadening of the MWD of the PPC formed, indicative of in situ chain transfer reactions (Chapter 2, Scheme 2.4). Furthermore, we suspected that the addition of a chain transfer agent under air-free conditions would initiate an *immortal polymerization*,[26] where the number of PPC chains formed is equal to the number of initiators and chain transfer agents present. We proceeded to apply catalyst system **2.3**/**3.1** to the *rac*-PO/CO_2 copolymerization while using the chain transfer agent *p*-trifluoromethylbenzoic acid (TFMBA) with an overall [PO]:[TFMBA]:[**2.3**]:[[PPN]Cl] loading of 2000:10:1:1 (Scheme 3.4). As there are a total of 12 initiators and/or chain transfer agents per cobalt catalyst, we expected that the PPC formed would have a M_n value of $1/12^{th}$ the theoretical M_n while maintaining a narrow MWD. After 43% conversion to PPC, we observed a M_n of 6.7 kg/mol with a MWD of 1.08. Notably, the corresponding calculated M_n value is equal to 87.7 kg/mol, which is 13 times that of the observed M_n value. In addition, both the pentafluorobenzoate and the *p*-trifluoromethyl end groups were observed using ^{19}F NMR spectroscopy (δ -64.11, -139.04, -149.40, -161.69) indicating that the

catalyst axial ligand, the anion from the $[PPN]^+$-based cocatalyst, and the chain transfer agent are capable of initiation.

The MWD of the PPC formed using catalyst system **2.3**/**3.1** in the presence of TFMBA is monomodal and very narrow. This suggests that the rate of chain transfer exceeds the rate of propagation. Specifically, ratio of the of chain-transfer and propagation rate constants (k_{tr}/k_p) can be approximated from the degree of polymerization[27] ($DP = (M_n/102$ g/mol)) with ($DP_n = 66$) and without ($DP_{n0} = 509$) chain transfer agents present for a given concentration of *rac*-PO ([M] = 14.3 mM) and TFMBA ([T] = 0.0715 mM) (Equation 3.2). In this case, we approximate $k_{tr}/k_p = 2.6$ which is consistent with the narrow MWDs that we observe.

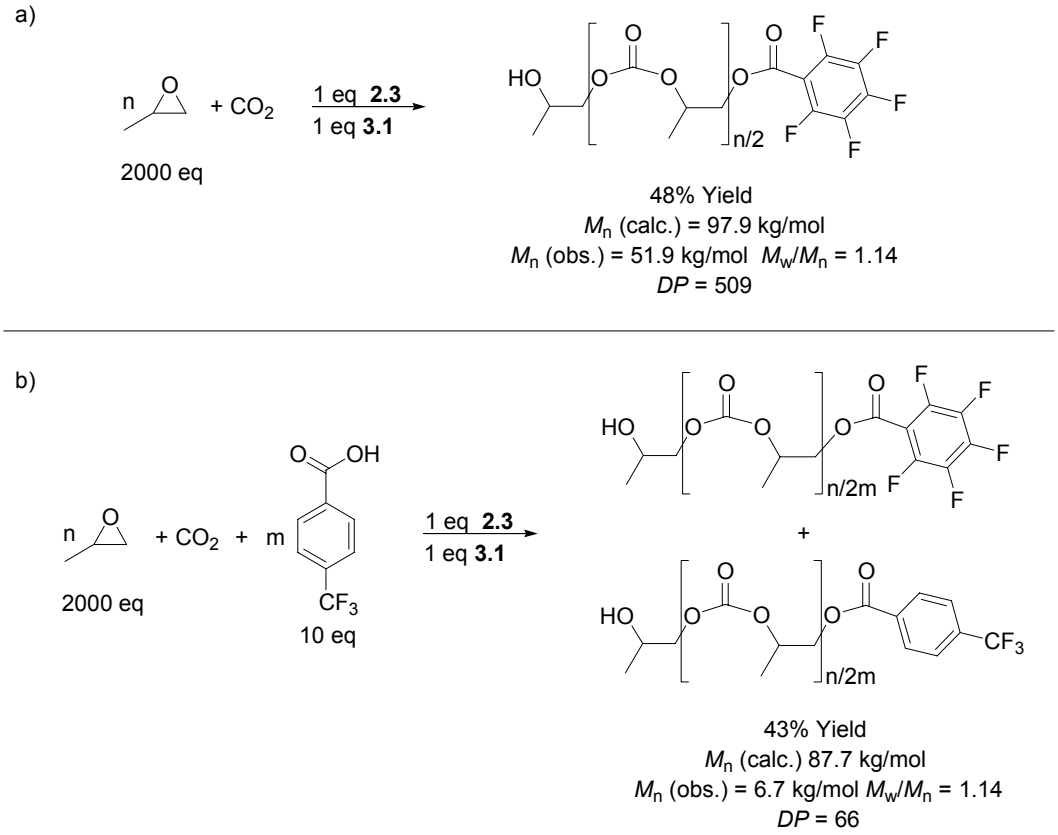

Scheme 3.4. Immortal-type behavior of (salen)CoX catalysts. (*R,R*)-(Salen-**1**)CoOBzF$_5$ (**2.3**)/[PPN][OBzF$_5$] (**3.1**) catalyzed *rac*-PO/CO_2 copolymerization a) without and b) with chain-transfer agent *p*-trifluoromethylbenzoic acid.

(Eq. 3.2.) $$DP_n^{-1} = DP_{n0}^{-1} + (k_{tr}/k_p)[T][M]^{-1}$$

k_{tr}/k_p = ratio of the of chain-transfer and propagation rate constants,
DP_n = degree of polymerization with chain-transfer agents present,
DP_{n0} = degree of polymerization without chain-transfer agents present,
[M] = monomer concentration [T] = chain-transfer agent concentration

3.4 Alteration of salen ligand

We have previously described that the nature of the salen ligand for (salen)CoX (X = halide or carboxylate) catalyzed PO/CO_2 copolymerization has a large influence on catalyst performance. As we have shown that the (salen)CoX/[PPN] systems behave differently from the (salen)CoX catalysts alone for PO/CO_2 copolymerization, we proceeded to carry out an independent study relating the salen ligand structure to (salen)CoX/[PPN]Cl catalyst performance.

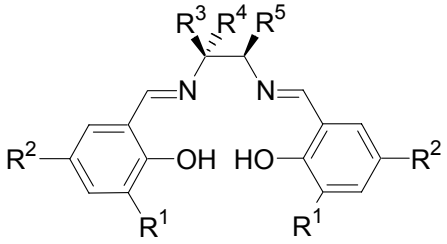

Ligand		R^1	R^2	R^3	R^4	R^5
(*R,R*)-(salen-**1**)H_2	(**2.6**)	^{t}Bu	^{t}Bu	H	(*R,R*)-*trans* -$(CH_2)_4$-	
rac-(salen-**1**)H_2	(**2.7**)	^{t}Bu	^{t}Bu	H	*rac-trans* -$(CH_2)_4$-	
(salen-**3**)H_2	(**2.9**)	^{t}Bu	^{t}Bu	H	H	H
(salen-**4**)H_2	(**2.10**)	^{t}Bu	^{t}Bu	Me	Me	H
(*R,R*)-(salen-**5**)H_2	(**2.11**)	^{t}Bu	^{t}Bu	H	(*R*)-Ph	*trans*-(*R*)-Ph
(*R,R*)-(salen-**8**)H_2	(**2.14**)	^{t}Bu	Br	H	(*R,R*)-*trans* -$(CH_2)_4$-	
(*R,R*)-(salen-**11**)H_2	(**2.17**)	cumyl	cumyl	H	(*R,R*)-*trans* -$(CH_2)_4$-	

Figure 3.7. Salen ligands used to synthesize (salen)$CoOBzF_5$ complexes. Cumyl = α,α'-dimethylbenzyl.

Table 3.6. Effect of catalyst structure: (salen)$CoOBzF_5$/[PPN]Cl catalyzed *rac*-PO/CO_2 copolymerization.[a]

Entry	Catalyst		Time (h)	PPC Yield[b] (%)	TOF[c] (h^{-1})	Selectivity PPC:PC	M_n[d] (kg/mol)	M_w/M_n[d]	Head-to-Tail Linkages[e] (%)
1	(*R,R*)-(salen-**1**)$CoOBzF_5$	(**2.3**)	0.5	30	600	99:1	9.8	1.18	94
2	(salen-**3**)$CoOBzF_5$	(**3.3**)	1.0	26	260	93:7	13.3	1.13	96
3	(salen-**4**)$CoOBzF_5$	(**3.4**)	0.5	26	520	94:6	11.5	1.15	95
4	(*R,R*)-(salen-**5**)$CoOBzF_5$	(**3.5**)	0.5	20	400	99:1	12.7	1.13	94
5	(*R,R*)-(salen-**8**)$CoOBzF_5$	(**3.6**)	1.5	30	200	>99:1	11.7	1.16	95
6	(*R,R*)-(salen-**11**)$CoOBzF_5$	(**3.7**)	1.5	29	190	91:9	12.5	1.17	93

[a] Copolymerizations run neat with [*rac*-PO]:[Co]:[[PPN]Cl] = 1000:1:1 at 22 °C with 100 psi of CO_2. All PPC contains ≥ 99% carbonate linkages as determined by ^{1}H NMR spectroscopy ($CDCl_3$, 300 MHz). [b] Based on isolated PPC yield. [c] Turnover frequency for PPC = (mol PO/(mol Co · h)). [d] Determined by GPC calibrated with polystyrene standards in THF at 40 °C. [e] Determined by quantitative $^{13}C\{^1H\}$ NMR spectroscopy ($CDCl_3$, 125 MHz, d_1 = 10s).

The complete list of salen ligands used to synthesize (salen)CoOBzF$_5$ complexes for this study is presented in Figure 3.7. We first investigated the effects of alternating the diimine backbone of (salen)CoOBzF$_5$/[PPN]Cl catalyst on *rac*-PO/CO$_2$ copolymerization activity. Both (salen-**3**)CoOBzF$_5$ (**3.3**)/[PPN]Cl and (*R,R*)-(salen-**5**)CoOBzF$_5$ (**3.4**)/[PPN]Cl had reduced activity, as compared to **2.3**/[PPN]Cl (Table 3.6, entries 1, 2 and 4). These complexes appeared less soluble in *rac*-PO/CO$_2$ than **2.3**, likely contributing to differences in catalyst performance. Notably, the more soluble (salen-**4**)CoOBzF$_5$ (**3.5**) has similar activity to **2.3** with [PPN]Cl (entry 3). Thus, it appears that changes to the diimine backbone are reflected primarily in catalyst solubility which influences the observed catalyst activity.

The PPC generated using any of the (salen)CoOBzF$_5$/[PPN]Cl catalyst systems is highly regioregular with greater than 93% HT connectivity. In an effort to further increase PPC regioregularity, we altered the steric bulk of the *ortho* and *para* substituents on the phenolate of the salen ligands ((*R,R*)-(salen-**8**)CoOBzF$_5$ (**3.6**) and (*R,R*)-(salen-**11**)CoOBzF$_5$ (**3.7**)). Interestingly, even the sterically bulky **3.7**/[PPN]Cl catalyst system did not show significantly improved regioselectivity (entry 6). Furthermore, both **3.6**/[PPN]Cl and **3.7**/[PPN]Cl systems were less active for *rac*-PO/CO$_2$ copolymerization than **2.3**/[PPN]Cl (entries 5 and 6). Overall, catalyst **2.3** is the most active *rac*-PO/CO$_2$ copolymerization catalyst with [PPN]Cl cocatalyst, which we attribute to this complex having the optimal solubility properties under the polymerization conditions employed.

3.5 Cocatalyst role

3.5.1 Exchange of catalyst axial ligand and cocatalyst anion

Based on our observations that 1) both the catalyst axial ligand and the anion from the $[PPN]^+$-based cocatalyst are capable of initiation and 2) the amount of [PPN]Cl added influences the experimental M_n value of the PPC obtained, we suspected the we would observe similar behavior for (salen)CoX/[PPN]Y catalyzed *rac*-PO/CO_2 copolymerization when exchanging X and Y. The *rac*-PO/CO_2 copolymerization data using a series of (salen)CoX/[PPN]Y catalyst systems are listed in Table 3.7. As previously discussed, the **2.3**/[PPN]Cl catalyst system has a TOF of 600 h^{-1} for PPC (entry 4) when a [PO]:[Co]:[[PPN]Cl] loading of 1000:1:1 is applied. When the catalyst axial ligand and the cocatalyst anion are switched (**2.4**/**3.1**), catalyst activity decreases slightly and a small amount of PC is produced (entry 5). This suggests that catalyst activity and selectivity is not completely independent of the origin of the nucleophile/initiator used. When comparing the **2.5**/**3.1** and **2.3**/bis(triphenylphosphine)iminium bromide ([PPN]Br or **3.8**) systems, similar catalyst performance is observed, with TOFs of 400 and 420 h^{-1}, and a 78% and 80% selectivity for PPC over PC, respectively (entries 7 and 3). In this case the origin of the nucleophile/initiator used has only a small influence on catalyst activity and selectivity for PPC.

To determine the most efficient anion for overall catalyst performance, we proceeded to study a series of (salen)CoX/[PPN]X systems. As previously described, catalysts (salen)CoX/[PPN]Cl have relative activities where X = Br < Cl < $OBzF_5$. Furthermore, we expected similar results when applying the same anion for both the catalyst axial ligand and the anion of the $[PPN]^+$-based cocatalyst. The *rac*-PO/CO_2 copolymerization catalyzed by **2.3**/**3.1** is highly active, with a TOF of 720 h^{-1} and >99:1 selectivity for PPC over PC (Table 3.7 entry 2). Alternatively, **2.4**/[PPN]Cl

exhibited a TOF of 600 h^{-1} for the generation of PPC (entry 1), which is similar to that of the mixed **2.3**/[PPN]Cl system. Catalyst system **2.5**/**3.8** was the least active and selective for *rac*-PO/CO_2 copolymerization, with a TOF of 370 h^{-1} and only 65% selectivity for PPC over PC (entry 3). In summary, whether the (salen)CoX/[PPN]Cl or (salen)CoX/[PPN]X systems are applied, we observe an activity trend of X = Br < Cl < $OBzF_5$, where the **2.3**/**3.1** catalyst system is the most active catalyst we report.

Table 3.7. Effect of varying the catalyst axial ligand and the cocatalyst anion: (*R,R*)-(salen-**1**)CoX (X = $OBzF_5$ (**2.3**), Cl (**2.4**), Br (**2.5**))/[PPN]Y catalyzed *rac*-PO/CO_2 copolymerization.[a]

Entry	Catalyst	Cocatalyst		PPC Yield[b] (%)	TOF[c] (h^{-1})	Selectivity PPC:PC[d]
1	**2.4**	[PPN]Cl		30	600	97:3
2	**2.3**	[PPN][$OBzF_5$]	(**3.1**)	36	720	>99:1
3	**2.5**	[PPN]Br	(**3.8**)	18	370	65:35
4	**2.3**	[PPN]Cl		30	600	99:1
5	**2.4**	**3.1**		27	530	96:4
6	**2.3**	**3.8**		21	420	80:20
7	**2.5**	**3.1**		20	400	78:20

[a] Copolymerizations run neat with [*rac*-PO]:[Co]:[[PPN]Cl] = 1000:1:1 at 22 °C with 100 psi of CO_2 for 0.5 h. All PPC contains ≥ 98% carbonate linkages as determined by ^{1}H NMR spectroscopy ($CDCl_3$, 300 MHz). [b] Based on isolated PPC yield. [c] Turnover frequency for PPC = (mol PO/(mol Co · h)). [d] Selectivity for PPC over PC.

3.5.2 Addition of various organic-based, ionic cocatalysts

Our initial discovery that [PPN]Cl is an excellent cocatalyst for the **2.3** catalyzed *rac*-PO/CO_2 copolymerization led us to investigate other additives as cocatalysts for this reaction.[21] Table 3.8 presents the effect of various organic-based, ionic cocatalysts on catalyst activity and selectivity for PPC. At low CO_2 pressures and in the absence of cocatalyst, the **2.3** catalyzed *rac*-PO/CO_2 copolymerization yields only trace PPC after 24 h (entry 1). The addition of either **3.1**, [PPN]Cl, or **3.2** results in a dramatic increase in the *rac*-PO/CO_2 copolymerization rate (entries 1-4)

where the most active catalyst system, **2.3**/**3.1** achieves a TOF of 720 h^{-1} with greater than 99:1 selectivity for PPC over PC. Use of **3.8** (entry 5) results in a lower overall selectivity for PPC over PC which we attribute to the better leaving group ability Br^- when compared to Cl^- or benzoate. When tetraphenylborate ($[BPh_4]^-$) is applied, **2.3**/bis(triphenylphosphine)iminium tetraphenylborate ([PPN][BPh_4] or **3.9**) only trace PPC is formed after 24 hours (entry 6). Notably, this supports that a nucleophilic anion is necessary for copolymerization rate enhancement.

To investigate the influence of the cocatalyst's cation structure on the *rac*-PO/CO_2 copolymerization using catalyst **2.3**, we surveyed a series of organic-based, chloride-containing, ionic cocatalysts. Replacement of [PPN]Cl with tetraphenylphosphonium chloride ([Ph_4P]Cl) reduced the copolymerization rate only slightly (entry 7), indicating that an imine moiety is not required for an effective cocatalyst. Furthermore, when triphenyl(triphenylmethyl)phosphonium chloride ([Ph_3CPPh_3]Cl) is used, catalyst activities are on the order of those for the **2.3**/[PPN]Cl system (entry 8). Alternatively, methyltriphenylphosphonium chloride [Ph_3PMe]Cl or *n*-butyltriphenylphosphonium chloride ([Ph_3P(*n*-Bu)]Cl) are ineffective cocatalysts (entries 9 and 10), which we postulate is due to deprotonation, forming ylid compounds.

Interestingly, tetrakis[tris(dimethylamino)phosphoranylidenamino]phosphonim chloride, where the positive charge is localized on the phosphorous, proved to be a less rate-enhancing cocatalyst than [Ph_4P]Cl, [PPN]Cl, or [Ph_3CPPh_3]Cl (entry 11). As we suspect that the cocatalyst cation hinders backbiting reactions of the propagating species and/or impedes decomposition of the active catalyst, we rationalize that cations with a delocalized positive charge are most beneficial for the copolymerization,[25] due to their stabilization of the separated ion pair.

Table 3.8. (*R,R*)-(Salen-**1**)CoOBzF$_5$ (**2.3**) catalyzed *rac*-PO/CO_2 copolymerization with organic-based, ionic cocatalysts.[a]

Entry	Cocatalyst		Time (h)	PPC Yield[b] (%)	TOF[c] (h^{-1})	Selectivity PPC:PC	M_n[d] (kg/mol)	M_w/M_n[d]	Head-to-Tail Linkages[e] (%)
1	None		24.0	<1	NA	NA	NA	NA	NA
2	[PPN]Cl		0.5	30	600	99:1	9.8	1.18	94
3	[PPN][*p*-(CF_3)benzoate]	(**3.2**)	0.5	33	660	>99:1	19.6	1.15	95
4	[PPN][$OBzF_5$]	(**3.1**)	0.5	36	720	>99:1	15.9	1.16	94
5	[PPN]Br	(**3.8**)	0.5	21	415	80:20	8.7	1.19	94
6	[PPN][BPh_4]	(**3.9**)	24.0	<1	NA	NA	NA	NA	NA
7	[PPh_4]Cl		0.5	25	550	97:3	8.6	1.19	94
8	[Ph_3CPPh_3]Cl		0.5	30	600	>99:1	8.4	1.19	94
9	[PPh_3(Me)]Cl		10.0	16	16	98:2	5.6	1.26	91
10	[PPh_3(*n*-Bu)]Cl		10.0	30	30	>99:1	7.3	1.20	96
11	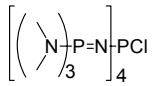		1.5	19	130	90:10	16.3	1.16	94
12	[*n*-Bu_4N]Cl		2.0	29	150	>99:1	6.6	1.15	93
13	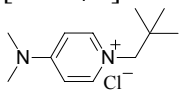		2.0	37	190	>99:1	11.7	1.19	94
14	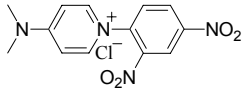	(**3.10**)	3.0	0	NA	NA	NA	NA	NA
15	[PPh_4]Br		0.5	24	480	96:4	16.4	1.15	94
16	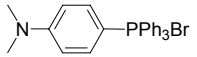	(**3.11**)	1.0	47	470	91:9	20.9	1.20	91

[a] Copolymerizations run neat with [*rac*-PO]:[**2.3**]:[cocatalyst] = 1000:1:1 at 22 °C with 100 psi of CO_2. All PPC contains ≥ 99% carbonate linkages. [b] Based on isolated PPC yield. [c] Turnover frequency for PPC = (mol PO/(mol Co · h)). [d] Determined by GPC calibrated with polystyrene standards in THF at 40 °C. [e] Determined by quantitative $^{13}C\{^1H\}$ NMR spectroscopy ($CDCl_3$, 125 MHz, d_1 = 10s).

Due to our success with phosphonium-based, ionic cocatalysts for *rac*-PO/CO_2 copolymerization, we continued to investigate a series of ammonium-based cations in an effort to likewise maximize the *rac*-PO/CO_2 copolymerization activity of catalyst **2.3**. Addition of *n*-tetrabutylammonium chloride ([*n*-Bu_4N]Cl) to the copolymerization afforded a TOF of 150 h^{-1} (entry 12), whereas use of *p*-*N,N*-dimethylamino-1-neopentylpyridinium chloride effected a TOF of 190 h^{-1} (entry 13). When *N,N*-dimethylamino-*p*-2,4-dinitrophenylpyridinium chloride (**3.10**) was used, however, no PPC was obtained (entry 14). We suspect that the nitro groups on this cocatalyst can coordinate to **2.3**, leading to its inactivation. Overall, use of ammonium-based, ionic cocatalysts is effective for *rac*-PO/CO_2 copolymerization however generally inferior to phosphonium alternatives.

Although we previously described cocatalyst **3.3** to effect a loss in selectivity for PPC over PC when compared to [PPN]Cl, when alternate phosphonium cations are used with Br^-, catalyst performance of **2.3** is improved. Interestingly, tetraphenylphosphonium bromide ([PPh_4]Br) or *p*-[(dimethylamino)phenyl]triphenylphosphonium bromide (**3.11**) are each more efficient cocatalysts than [PPN]Br with catalyst **2.3**, effecting TOFs of 480 h^{-1} and 470 h^{-1} respectively (entries 15 and 16). Additionally, selectivity for PPC over PC is increased in each case. Evidently, the overall activity and selectivity for PPC over PC is not solely influenced by the cation and anion used, but also on the specific combination of the two.

3.6 Synthesis of stereo- and regioregular PPC

The mechanistic insight obtained from the stereochemical experiments with **2.4** and *rac*-(salen-**1**)CoBr (**2.30**) led us to pursue similar studies with the **2.3**/[PPN]Cl catalyst systems. Table 3.9 lists the copolymerization data for **2.3**/[PPN]Cl and *rac*-(salen-**1**)$CoOBzF_5$ (**3.12**)/[PPN]Cl with *rac*-, (*S*)-, and (*R*)-PO/CO_2. Remarkably, the

addition of [PPN]Cl to the **2.3** catalyzed *rac*-PO/CO_2 copolymerization not only increases the catalytic activity, but also improves stereo- and regioselectivity. Specifically, **2.3**/[PPN]Cl demonstrates an activity of 620 turnovers per hour for the copolymerization of *rac*-PO and CO_2, affording iso-enriched PPC with 94% HT connectivity (Table 3.10, entry 1 and Figure 3.8a). The substitution of (*S*)- for *rac*-PO in this copolymerization results in a near doubling of the reaction rate (TOF = 1100 h^{-1}), affording highly alternating, isotactic PPC with 96% HT connectivity (Table 3.10, entry 2 and Figure 3.8b). Alternatively, the substitution of (*R*)- for *rac*-PO results in substantial rate inhibition with a TOF of only 210 h^{-1} (Table 3.10, entry 3 and Figure 3.8c). The product PPC from this reaction is isotactic, with 87% HT connectivity, demonstrating that the regioselectivity of this system is less dependent on the relative stereochemistry of PO and catalyst than was observed with **2.4** alone.

The copolymerization of (*R*)-PO/CO_2 with catalyst **3.12** and [PPN]Cl yields isotactic PPC with 95% HT connectivity (Table 3.10, entry 4 and Figure 3.8d). This polymer shows a monomodal GPC trace with a MWD of 1.07. Similar to that discussed above, this result supports a mechanism in which each propagating species can dissociate from the metal center during the copolymerization and is influenced by catalysts of both possible chiralities. Finally, using catalyst **3.12** with [PPN]Cl for the copolymerization of *rac*-PO and CO_2 yields atactic PPC with 95% HT connectivity (Table 3.9, entry 5 and Figure 3.8e). Unlike the corresponding results using catalyst **2.30** alone (Chapter 2), the PPC microstructures generated by **3.12**/[PPN]Cl or **2.3**/[PPN]Cl catalyst systems are essentially the same for the *rac*-PO/CO_2 copolymerization.

Table 3.9. (*R,R*)-(salen-**1**)CoOBzF$_5$ (**2.3**), *rac*-(salen-**1**)CoOBzF$_5$ (**3.12**) catalyzed PO/CO_2 copolymerization with cocatalyst [PPN]Cl using *rac*-, (*S*)-, and (*R*)-PO.[a]

Entry	Complex	PO	Time (h)	PPC Yield[b] (%)	TOF[c] (h^{-1})	Selectivity (%PPC)	M_n[d] (kg/mol)	M_w/M_n[d]	Head-to-Tail Linkages[e](%)
1	**2.3**	*rac*-	1.0	32	640	99	26.8	1.13	94
2	**2.3**	(*S*)-	0.5	27	1,100	>99	22.2	1.15	96
3	**2.3**	(*R*)-	2.0	21	210	98	19.1	1.12	87
4	**3.12**	(*R*)-	1.0	37	740	>99	34.5	1.07	95
5	**3.12**	*rac*-	1.0	33	650	>99	32.7	1.10	95

[a] Copolymerizations run neat with [PO]:[Co]:[(PPN)Cl] = 2000:1:1 at 22 °C with 200 psi of CO_2. All product PPC contains ≥ 98% carbonate linkages as determined by ^{1}H NMR spectroscopy ($CDCl_3$, 300 MHz). [b] Based on isolated PPC. [c] Turnover frequency for PPC = (mol PO/(mol Co · h)). [d] Determined by GPC calibrated with polystyrene standards in THF at 40 °C. [e] Determined by quantitative $^{13}C\{^1H\}$ NMR spectroscopy ($CDCl_3$, 125 MHz, d_1 = 10s).

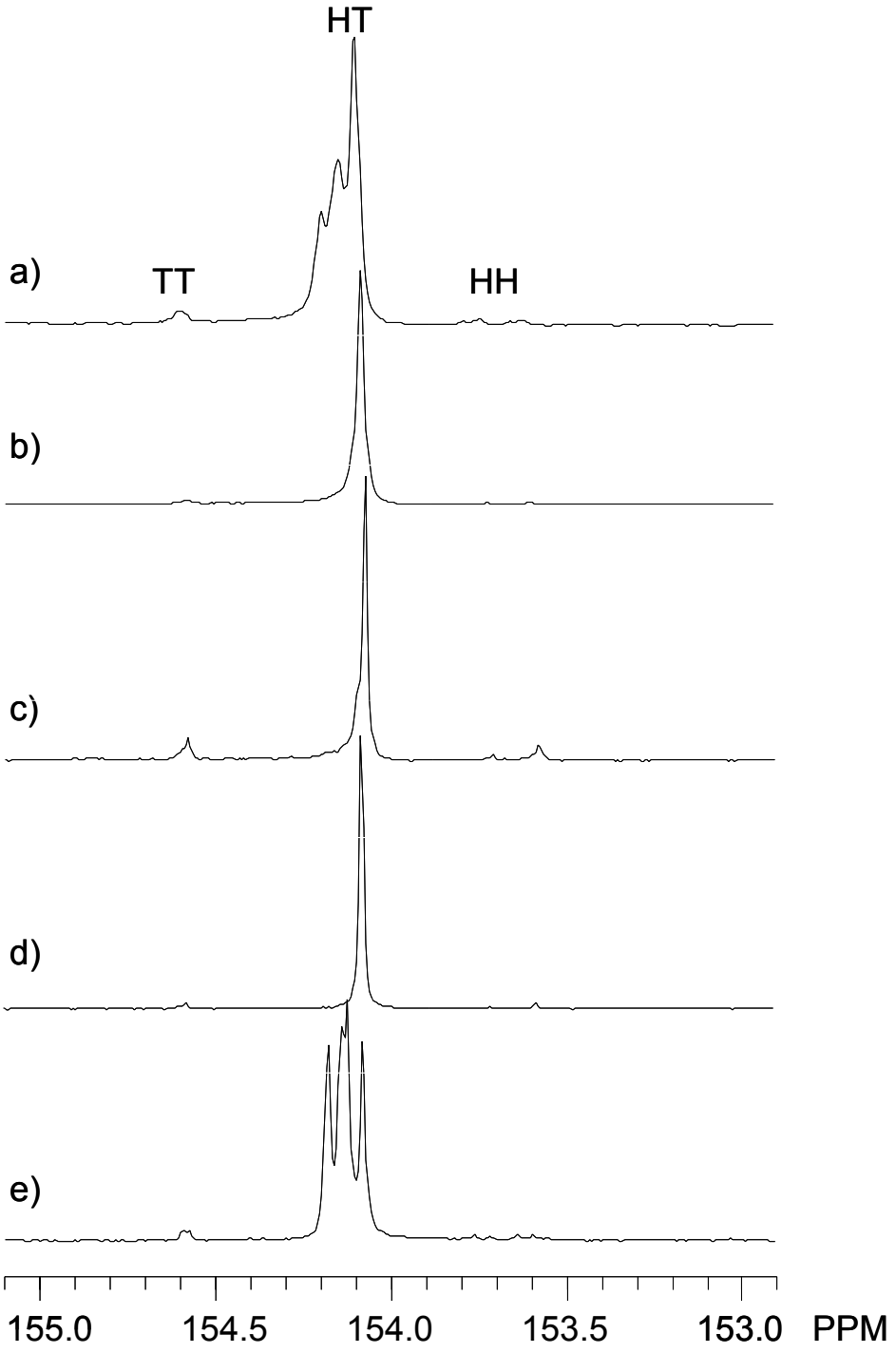

Figure 3.8. Carbonyl region of the quantitative $^{13}C\{^{1}H\}$ NMR spectra ($CDCl_3$, 125 MHz, d_1 = 10s) of PPC synthesized from (a) (*R,R*)-(salen-**1**)$CoOBzF_5$ (**2.3**) and *rac*-PO, (b) **2.3** and (*S*)-PO, (c) **2.3** and (*R*)-PO, (d) *rac*-(salen-**1**)$CoOBzF_5$ (**3.12**) and (*R*)-PO, and (e) **3.12** and *rac*-PO. In all cases, cocatalyst [PPN]Cl was used.

3.7 Mechanistic hypothesis

Our studies concerning (salen)CoX/[PPN]Y catalyzed PO/CO_2 copolymerization have revealed that the both the catalyst axial ligand (X) and the cocatalyst anion (Y) can be found as end-groups on the PPC formed. Additionally, we observe a non-linear inverse relationship between the amount of [PPN]Cl cocatalyst added and the M_n value of the PPC obtained. Finally, we have seen similar catalyst performance when comparing (salen)CoX/[PPN]Y to (salen)CoY/[PPN]X in the case where $X \neq Y$. Based on these results, we hypothesize that both the catalyst axial ligand and the cocatalyst anion are capable of initiation, and that two polymer chains can simultaneously propagate from either side of the cobalt-salen plane (Scheme 3.5); a mechanism similar to that proposed by Inoue and coworkers using aluminum porphyrins and ammonium and phosphonium-based cocatalysts.[10, 11, 17-19] Furthermore, we put forth a mechanism where the propagating carboxylate dissociates from the cobalt center during the copolymerization prior to PO ring-opening and can also exchange with the anion from the organic-based, ionic cocatalyst. In the event that more than one equivalent of cocatalyst is applied, all cocatalyst anions present are capable of PPC initiation.

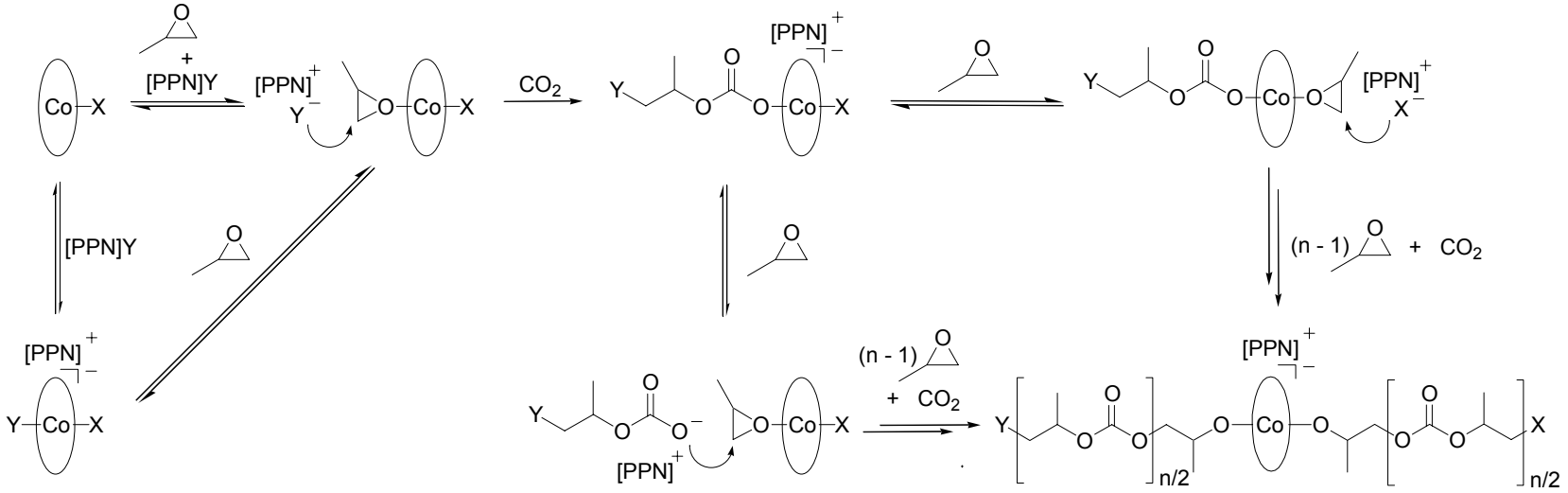

Scheme 3.5. Proposed mechanism for *rac*-PO/CO_2 copolymerization using catalyst system **2.3**/[PPN]Y (X, Y = halide or carboxylate).

3.8 Addition of Lewis-basic cocatalysts

The addition of Lewis basic cocatalysts to epoxide/CO_2 copolymerization with porphyrin or salen-type metal catalysts has provided for enhanced catalytic activities in a variety of systems.[2, 4-7, 13-16, 21-24] Likewise, we investigated a series of Lewis basic cocatalysts when added to the **2.3** catalyzed *rac*-PO/CO_2 copolymerization. We initially suggest a mechanism where the Lewis basic cocatalyst reversibly coordinates to the cobalt, increases the electron density on the metal, and labilizes the *trans* species to it (Scheme 3.6). This scheme, where a more electron rich metal center is more efficient for epoxide/CO_2 copolymerization, is in accordance with previously proposed mechanisms in similar systems.[2, 4-7, 15, 22, 23, 28] In conjunction with **2.3**, triethylamine and *n*-trioctylamine are effective cocatalysts achieving TOFs of 190 h^{-1} and 175 h^{-1}, respectively (Table 3.9, entries 1 and 2). The similarity in activity suggests that the alkyl length of the amine cocatalyst has little influence on its reactivity. Interestingly, when increasing relative amounts of *n*-trioctylamine are applied, the M_n values of the resultant PPCs decrease (Figure 3.9). This is consistent with the Lewis basic cocatalyst capable of initiation and/or reacting with CO_2, a scheme similar to that proposed by Darensbourg (Scheme 3.7b)[13] and Lu (Scheme 3.7a).[21]

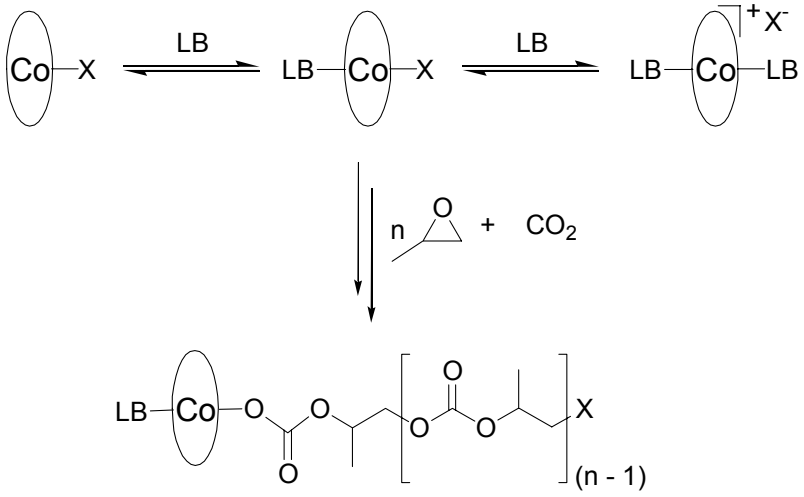

Scheme 3.6. A mechanism for (*R,R*)-(salen-**1**)CoOBzF_5 (**2.3**) catalyzed PO/CO_2 copolymerization using Lewis basic (LB) cocatalysts (X = OBzF_5 or polymer).

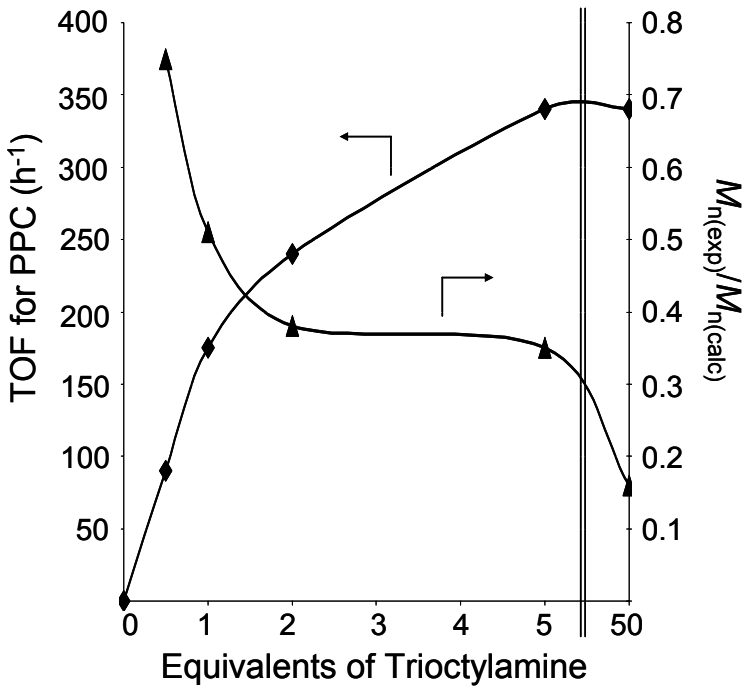

Figure 3.9. Effect of trioctylamine loading on (*R,R*)-(salen-**1**)CoOBzF$_5$ (**2.3**) catalyzed *rac*-PO/CO_2 copolymerization activity and M_n values of the PPC formed. Copolymerizations run neat with [*rac*-PO]:[Co] = 1000:1 at 22 °C with 100 psi of CO_2 and carried out to < 40% conversion. Turnover frequency for PPC = (mol PO/(mol Co · h)). $M_{n(exp)}/M_{n(calc)}$ = ratio of the experimental M_n value to the corresponding calculated M_n value.

When perfluorotriethylamine ($N(CF_2CF_3)_3$) is applied, **2.3** has no copolymerization activity (entry 3), presumably due to the very weak Lewis basicity of this cocatalyst. With triphenylamine (NPh_3) or tricyclohexylphosphine (PCy_3) cocatalysts, little or no copolymerization activity is realized (entries 4 and 5), attributable to poor coordination of these sterically bulky Lewis bases. Additionally, the use of triphenyl phosphine (PPh_3), pyridine or 4-dimethylaminopyridine (DMAP) cocatalysts with **2.3** shows little overall activity (entries 6, 7 and 8). These cocatalysts

are capable of irreversible coordination to the cobalt catalyst leading to its inactivation.

Overall, a delicate interplay between Lewis basicity, steric bulk, and reversibility of coordination make the electron rich alkyl amines the most effective Lewis basic cocatalysts, although they are inferior to the organic-based, ionic cocatalysts $[Ph_4P]Cl$, $[PPh_3CPh_3]Cl$ or [PPN]Y (Y = Cl or carboxylate). Furthermore, we suspect that both the coordination of the Lewis base to the metal center (Scheme 3.6), and/or initiation is viable (Scheme 3.7) where a competition between mechanisms is determined by the steric and electronic environment around the cocatalyst donor atom.

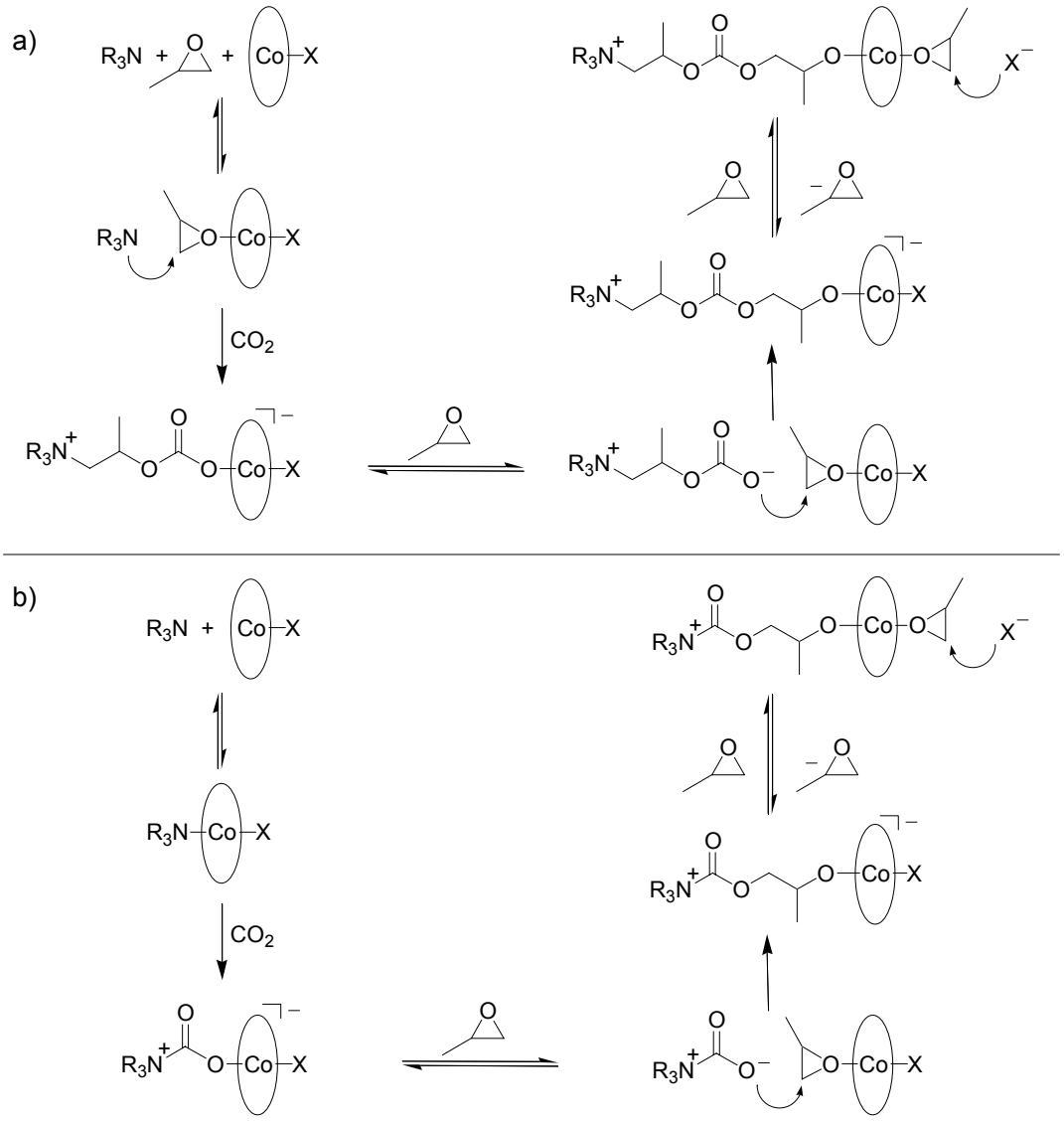

Scheme 3.7. A Mechanism for (salen)CoX (X = halide or carboxylate) catalyzed *rac*-PO/CO_2 copolymerization in the presence of a Lewis base cocatalyst (NR_3, R = alkyl): a) The Lewis base directly ring-opens the cobalt-bound PO and b) Insertion of CO_2 into the Co-N bond prior to PO ring-opening.

Table 3.10. (*R,R*)-(Salen-**1**)CoOBzF$_5$ (**2.3**) catalyzed *rac*-PO/CO_2 copolymerization with Lewis basic cocatalysts.[a]

Entry	Cocatalyst	PPC Time (h)	PPC Yield[b] (%)	TOF[c] (h^{-1})	Selectivity PPC:PC	M_n[d] (kg/mol)	M_w/M_n[d]	Head-to-Tail Linkages (%)[e]
1	$N(CH_2CH_3)_3$	2	38	190	>99:1	18.5	1.17	94
2	$N((CH_2)_7CH_3)_3$	2	35	175	>99:1	18.1	1.14	93
3	$N(CF_2CF_3)_3$	24	0	NA	NA	NA	NA	NA
4	NPh_3	24	0	NA	NA	NA	NA	NA
5	PCy_3	24	24	10	99:1	13.0	1.14	93
6	PPh_3	10	23	29	>99:1	5.0	1.13	92
7	Pyridine	10	13	13	>99:1	5.6	1.17	92
8	DMAP	10	11	11	99:1	5.9	1.16	93

[a] Copolymerizations run neat with [*rac*-PO]:[**2.3**]:[cocatalyst] = 1000:1:1 at 22 °C with 100 psi of CO_2. All PPC contains ≥ 99% carbonate linkages.[b] Based on isolated PPC yield. [c] Turnover frequency for PPC = (mol PO/(mol Co · h)). [d] Determined by GPC calibrated with polystyrene standards in THF at 40 °C. [e] Determined by quantitative ^{13}C {^1H} NMR spectroscopy ($CDCl_3$, 125 MHz, d_1 = 10s).

3.9 Conclusions

We have investigated a series of cobalt-based, salen-supported catalysts with organic-based, ionic and Lewis basic cocatalysts for the copolymerization of PO and CO_2. Through adjustment of the reaction environment and catalyst optimization we maximized catalytic activity and selectivity for the generation of highly alternating, regioregular PPC with controlled molecular weight and minimal PC byproduct. Through variation of the catalyst axial ligand and the anionic component of the cocatalyst, we observe each of these species as PPC end-groups. The influence of a series of organic-based, ionic and Lewis basic cocatalysts on catalyst performance of **2.3** was explored. Overall, catalyst **2.3** with $[Ph_4P]Y$ (Y = Cl or Br), $[PPh_3CPh_3]Cl$ or [PPN]Y (Y = Cl or pentafluorobenzoate) cocatalysts were the most successful, exhibiting TOFs up to 720 h^{-1} for *rac*-PO/CO_2 copolymerization, and producing PPC with greater than 94% HT connectivity. By varying catalyst and PO stereochemistry,

we observed pronounced alterations in the resultant PPC microstructure, as well as changes in catalytic activity. The copolymerization of (*S*)-PO and CO_2 with catalyst **2.3** and cocatalyst [PPN]Cl has a TOF = 1100 h^{-1} for isotactic PPC. To our knowledge, these catalyst systems exhibit the highest activities for the copolymerization of PO and CO_2, as well as maintain excellent polymer regioselectivity and molecular weight control.

3.10 Experimental section

3.10.1 General procedures

All air or water sensitive reactions were carried out under dry nitrogen using an MBraun Labmaster drybox or standard Schlenk-line techniques. Methylene chloride and diethyl ether were dried and degassed by passing through a column of activated alumina and by sparging with dry nitrogen. (*S,S*)- and (*R,R*)-*N,N′*-bis(3,5-di-*tert*-butylsalicylidene)-1,2-diaminocyclohexanecobalt(II) ((*S,S*)-(salen-**1**)Co^{II}, (*R,R*)-(salen-**1**)Co^{II}) were purchased from Aldrich and recrystallized from methylene chloride and methanol. PO was dried over calcium hydride and vacuum transferred before use. (*R*)- and (*S*)-PO were obtained using kinetic resolution as described by Jacobsen and coworkers.[29] CO_2 (99.998% purity) was purchased from Airgas and passed over a column of 4Å molecular sieves. All other reagents were purchased from commercial sources and used as received. Degradation of PPC to PC was performed according to literature procedure[30] and the product PC was analyzed by gas chromatography. Gas chromatograms were obtained on a Hewlett-Packard 6890 series gas chromatograph using a beta-DEX 225 chiral capillary column (30.0 m x 250 μm x 0.25 μm nominal), a flame ionization detector, and He carrier gas. Varian Mercury (^{1}H NMR, 300 MHz), Varian Inova (^{1}H NMR, 500 MHz; $^{13}C\{^1H\}$ NMR, 125 MHz; ^{19}F NMR, 470 MHz) spectrometers were used to record $^{13}C\{^1H\}$, ^{19}F, and ^{1}H NMR spectra, which were referenced versus residual nondeuterated solvent shifts. C_6F_6 (–

162.90 ppm) was used as a reference for all ^{19}F NMR spectra. Quantitative $^{13}C\{^{1}H\}$ NMR spectroscopy ($CDCl_3$, 125 MHz, d_1 = 10s) was used for integration of the carbonyl region of PPC (t_1 = 1.5s). GPC analyses were carried out using a Waters instrument (M515 pump, U6K injector) equipped with Waters UV486 and Waters 2410 differential refractive index detector, and four 5 μm PL Gel columns (Polymer Laboratories; 100 Å, 500 Å, 1000 Å, and Mixed C porosities) in series. The GPC columns were eluted with THF at 40 ºC at 1 mL/min and were calibrated using 23 monodisperse polystyrene standards. Elemental analyses were carried out by Robertson Microlit Laboratories in Madison, N.J. IR spectra were measured on a Mattson Research Series FTIR. High resolution mass spectra were obtained from the Mass Spectrometry Laboratory, School of Chemical Sciences, University of Illinois. All (salen)CoX complexes reveal axial ligand (X) loss in the (EI) mass spectra attributable to the poor stability of this complex under the applied conditions. In the case of all (salen)CoOBzF_5 complexes, carbons on the phenyl group of pentafluorobenzoate were not assigned in the $^{13}C\{^{1}H\}$ NMR spectra due to complex carbon fluorine splitting patterns.

3.10.2 Representative PO/CO_2 copolymerization (CTC-4-115). A 100 mL Parr autoclave was heated to 120 °C under vacuum for 4 h, then cooled under vacuum to 22 °C and moved to a drybox. Complex **2.3** (11.7 mg, 0.0143 mmol), cocatalyst [PPN]Cl (8.2 mg, 0.014 mmol) and *rac*-PO (2.00 mL, 28.6 mmol) were placed in a glass sleeve with a Teflon stir bar inside the Parr autoclave. The autoclave was pressurized to 200 psi of CO_2 and was left to stir at 22 °C for 2 h. The reactor was vented at 22 °C. A small aliquot of the resultant polymerization mixture was removed from the reactor for ^{1}H NMR and GPC analysis. The remaining polymerization mixture was then dissolved in methylene chloride (5 mL), quenched with 5% HCl solution in methanol (0.2 mL), and transferred to a pre-weighed vial. The product

mixture was dried *in vacuo* to constant weight, and the crude yield was determined after subtracting out the catalyst weight (1.5 g, 52%). The product was dissolved in methylene chloride (3 mL) and precipitated from methanol (30 mL). The polymer was collected and dried *in vacuo* to constant weight, and the polymer yield was determined (1.4 g, 49%).

3.10.3 Synthesis of ligand precursors. The synthetic procedures for (*R,R*)-(salen-**1**)H_2 (**2.6**), *rac*-(salen-**1**)H_2 (**2.7**), (salen-**3**)H_2 (**2.9**), (salen-**4**)H_2 (**2.10**), (*R,R*)-(salen-**5**)H_2 (**2.11**), (*R,R*)-(salen-**8**)H_2 (**2.14**), and (*R,R*)-(salen-**11**)H_2 (**2.17**) have been previously described in Chapter 2.

3.10.4 Synthesis of (salen)Co precursors. The synthetic procedures for (*R,R*)-(salen-**1**)Co, *rac*-(salen-**1**)Co, (salen-**3**)Co (**2.21**), (salen-**4**)Co, (*R,R*)-(salen-**5**)Co, (*R,R*)-(salen-**8**)Co, and (*R,R*)-(salen-**11**)Co, have been previously described in Chapter 2.

3.10.5 Synthesis of (salen)CoX Complexes. The synthetic procedures for (*R,R*)-(salen-**1**)CoOAc (**2.1**), (*R,R*)-(salen-**1**)CoOBzF_5 (**2.3**), (*R,R*)-(salen-**1**)CoCl (**2.4**), and (*R,R*)-(salen-**1**)CoBr (**2.5**) have been previously described in Chapter 2. The synthesis and characterization of all new (salen)CoX complexes are described below:

***rac*-(Salen-1)CoOBzF_5 (3.11, CTC-4-218).** Recrystallized *rac*-(salen-**1**)Co (0.5 g, 0.8 mmol) and pentafluorobenzoic acid (0.18 g, 0.83 mmol) were added to a 50 mL round-bottomed flask charged with a Teflon stir bar. Toluene (20 mL) was added to the reaction mixture, and it was stirred open to air at 22 °C for 12 h. The solvent was removed by rotary evaporation at 22 °C, and the solid was suspended in 200 mL of pentane and filtered. The dark green crude material was dried *in vacuo* and collected (0.60g, 89%). ^{1}H NMR (DMSO-d_6, 500 MHz): δ 1.30 (s, 18H), 1.59 (m, 2H), 1.74 (s, 18H), 1.90 (m, 2H), 2.00 (m, 2H), 3.07 (m, 2H), 3.60 (m, 2H), 7.44 (s,

2H), 7.47 (s, 2H), 7.81 (s, 2H). $^{13}C\{^{1}H\}$ NMR (DMSO-d_6, 125 MHz): δ 24.33, 29.56, 30.35, 31.47 31.52, 33.50, 35.76, 69.38, 118.57, 128.74, 129.26, 135.79, 141.78, 162.18, 164.64. ^{19}F NMR (DMSO-d_6, 470 MHz): δ –166.20 (m), –162.37 (m), –144.46 (m).

(Salen-3)CoOBzF$_5$ (3.4, NOV-3-19). (Salen-**3**)Co (420 mg, 0.76 mmol) and pentafluorobenzoic acid (280 mg, 1.3 mmol) were added to a 50 mL round-bottomed flask with a Teflon stir bar. To it was added 10 mL of toluene and the mixture was stirred at 22 °C open to air for 12 h. The toluene was removed *in vacuo* and the brown residue was suspended in pentane and filtered. Following the removal of solvent, the black solid (salen-**3**)CoOBzF$_5$ was obtained (370 mg, 63%). ^{1}H NMR (DMSO-d_6, 500 MHz): δ 1.30 (s, 18H), 1.73 (s, 18H), 4.14 (s, 4H), 7.31 (s, 2H), 7.44 (s, 2H), 8.12 (s, 2H). $^{13}C\{^{1}H\}$ NMR (DMSO-d_6, 125 MHz): δ 30.27, 31.43, 33.39, 35.75, 58.28, 118.41, 128.26, 128.71, 135.82, 141.97, 162.37, 168.60. ^{19}F NMR (DMSO-d_6, 470 MHz): δ -162.10, -157.93, -142.66.

(**Salen-4)CoOBzF$_5$ (3.6, CTC-4-162).** (Salen-**4**)Co (260 mg, 0.45 mmol) and pentafluorobenzoic acid (95 mg, 0.45 mmol) were added to a 50 mL round-bottomed flask with a Teflon stir bar. To it was added 10 mL of toluene and the mixture was stirred at 22 °C open to air for 12 h. The toluene was removed *in vacuo* and the solid was dissolved in pentane and filtered. Following the removal of solvent *in vacuo*, the product (salen-**4**)CoOBzF$_5$ was obtained (230 mg, 65%). ^{1}H NMR (DMSO-d_6, 500 MHz): δ 1.30 (s, 9H), 1.31 (s, 9H), 1.62 (s, 6H), 1.73 (s, 18H), 4.02 (s, 2H), 7.35 (s, 1H), 7.47 (s, 3H), 7.87 (s, 1H), 8.02 (s, 1H). $^{13}C\{^{1}H\}$ NMR (DMSO-d_6, 125 MHz): δ 26.87, 30.12, 30.31, 31.36, 31.41, 33.24, 33.32, 35.55, 35.59, 118.15, 119.29, 127.80, 128.53, 128.69, 129.06, 135.55, 137.51, 141.25, 141.83, 166.10, 168.15. ^{19}F NMR (DMSO-d_6, 470 MHz): δ -163.00, -161.31, -144.06.

(*R,R*)-(Salen-5)CoOBzF$_5$ (3.5, CTC-4-287). To a 50 mL round-bottomed flask charged with a Teflon stirbar was added (*R,R*)-(salen-**5**)Co (0.20 g, 0.29 mmol), pentafluorobenzoic acid (62 mg, 0.29 mmol) and toluene (10 mL). The mixture was stirred open to air for 12 h at 22 °C. The toluene was removed by rotary evaporation and the crude solid was washed with pentane (50 mL), filtered, and dried *in vacuo* to afford a green solid (0.19 g, 72%). ^{1}H NMR (DMSO-d_6, 500 MHz): δ 1.22 (s, 18H), 1.76 (s, 18H), 5.62 (s, 2H), 6.97 (s, 2H), 7.23 (s, 2H), 7.41- 7.48 (m, 12H). ^{13}C{^{1}H} NMR (DMSO-d_6, 125 MHz): δ 30.38, 31.35, 33.40, 35.80, 76.64, 117.59, 128.69, 129.24, 129.96, 134.87, 136.16, 141.97, 162.34, 166.67. ^{19}F NMR (DMSO-d_6, 470 MHz): δ -163.66, -162.81, -144.85. HRMS (EI) *m/z* calcd. ($C_{51}H_{54}CoF_5N_2O_4$ – $C_7F_5O_2$) 701.3517, found 701.3533.

(*R,R*)-(salen-8)CoOBzF$_5$ (3.7, CTC-4-151). The procedure for the synthesis of (salen-**3**)CoOBzF$_5$ was applied to the synthesis of (*R,R*)-(salen-**8**)CoOBzF$_5$; however, (*R,R*)-(salen-**8**)Co (250 mg, 0.39 mmol) and pentafluorobenzoic acid (83 mg, 0.39 mmol) in 10 mL of toluene were used to afford the product (*R,R*)-(salen-**8**)CoOBzF$_5$ (280 mg, 83%). ^{1}H NMR (DMSO-d_6, 500 MHz): δ 1.60 (m, 2H), 1.70 (s, 18H), 1.87 (m, 2H), 1.99 (m, 2H), 3.02 (m, 2H), 3.60 (m, 2H), 7.37 (d, ^4J = 2.0 Hz, 2H), 7.77 (d, ^4J = 2.0 Hz, 2H), 7.95 (s, 2H). ^{13}C{^{1}H} NMR (DMSO-d_6, 125 MHz): δ 24.02, 29.57, 29.79, 35.75, 69.48, 104.92, 120.69, 133.41, 135.00, 145.07, 163.13, 164.19. ^{19}F NMR (DMSO-d_6, 470 MHz): δ -163.19, -162.39, -144.39.

(*R,R*)-(salen-11)CoOBzF$_5$ (3.8, CTC-4-153). Employing the same reaction conditions as for (*R,R*)-(salen-**5**)CoOBzF$_5$, (*R,R*)-(salen-**11**)Co (0.25 g, 0.29 mmol) and pentafluorobenzoic acid (62 mg, 0.29 mmol) were used to afford the crude green product (0.21 g, 68%). ^{1}H NMR (DMSO-d_6, 500 MHz): δ 1.48 (m, 2H), 1.57 (s, 6H), 1.58 (s, 6H), 1.75 (s, 6H), 1.85 (m, 2H), 1.94 (m, 2H), 2.29 (s, 6H), 2.92 (m, 2H), 3.38 (m, 2H), 6.98 (s, 2H), 7.07 (t, ^3J = 7.0 Hz, 2H), 7.12 – 7.28 (m, 18H), 7.45 (d, ^4J = 2.5

Hz, 2H), 7.76 (s, 2H). $^{13}C\{^{1}H\}$ NMR (DMSO-d_6, 125 MHz): δ 24.09, 28.80, 29.45, 30.19, 30.30, 32.47, 41.33, 43.25, 68.96, 118.82, 124.97, 125.23, 126.06, 127.63, 127.76, 130.71, 132.90, 135.03, 140.90, 150.61, 151.10, 161.80, 164.61. ^{19}F NMR (DMSO-d_6, 470 MHz): δ -163.66, -162.78, -144.92. HRMS (EI) *m/z* calcd ($C_{63}H_{60}CoF_5N_2O_4 - C_7F_5O_2$) 851.3987, found 851.3984.

3.10.6 Cocatalyst synthesis. Bis(triphenylphosphine)iminium chloride ([PPN]Cl), bis(triphenylphosphine)iminium bromide ([PPN]Br), tetraphenylphosphonium chloride ([PPh_4]Cl), triphenyl(triphenylmethyl)phosphonium chloride ([Ph_3CPPh_3]Cl), methyltriphenylphosphonium chloride ([PPh_3(Me)]Cl), and *n*-butyltriphenylphosphonium chloride [PPh_3(*n*-Bu)]Cl are commercially available and were recrystallized from dry methylene chloride and dry diethyl ether and dried *in vacuo* for 12 h prior to use. Triethyl amine was dried over CaH_2 and vacuum transferred prior to use. 4-Dimethylamino-1-neopentylpyridinium chloride, triphenylphosphine, triphenylamine, tricyclohexylphosphine, *n*-tetrabutylammonium chloride ([*n*-Bu_4N]Cl), 4-dimethylaminopyridine (DMAP), and trioctylamine are commercially available and were dried *in vacuo* for 12 h prior to use. Pyridine and perfluorotriethylamine ($N(CF_2CF_3)_3$) are commercially available and were used as received. [*p*-(Dimethylamino)phenyl]triphenylphosphonium bromide (**3.11**) (**CTC-5-048**) was prepared following literature procedures[31] and was precipitated from dry methylene chloride and dry diethyl ether and dried *in vacuo* for 12 h prior to use. *N,N*-Dimethylamino-*p*-2,4-dinitrophenylpyridinium chloride (**3.10**) (**NOV-3-093**) was prepared following literature procedures[32] and was dried *in vacuo* for 12 h prior to use.

Bis(triphenylphosphine)iminium bromide (3.3, [PPN]Br, NOV-3-76). [PPN]Cl (200 mg, 0.348 mmol) was dissolved in methylene chloride (20 mL) and was added to a 250 mL separatory funnel. The solution was then shaken thoroughly with 4 x 50 mL of a saturated NaBr solution in water, and then with 2 x 50 mL distilled

water. The organic layer was collected and decanted from any residual water, and dried by rotary evaporation to yield crude [PPN]Br. Precipitation from dry methylene chloride and diethyl ether under N_2 afforded a white solid which was in agreement with literature characterization (mp 252 – 254 °C) [ref. 253-254 °C].[25]

Bis(triphenylphosphine)iminium *p*-trifluoromethylbenzoate (3.2, NOV-3-204). NaOH (75 mg, 1.9 mmol) and *p*-trifluoromethylbenzoic acid (360 mg, 1.9 mmol) were added to a 50 mL round-bottomed flask (A) charged with a Teflon stir bar. Distilled H_2O (10 mL) was added to the reaction mixture and it was stirred at 22 °C until all was dissolved. In a second 50 mL round-bottom flask (B) charged with a Teflon stir bar was added [PPN]Cl (220 mg, 0.37 mmol) and distilled H_2O and the mixture was heated to 80 °C until all was dissolved. Solution A was then filtered (to remove any unreacted starting material) and was added to solution B at 80 °C and was allowed to heat at 80 °C for 30 min. The cloudy solution was cooled to 22 °C, and the product was extracted into methylene chloride in a separatory funnel, and washed with distilled H_2O. The methylene chloride layer was collected and decanted from any residual H_2O. The methylene chloride was removed *in vacuo* and the white solid was recrystallized from dry methylene chloride and diethyl ether under N_2 to afford white needles (100 mg, 37%). ^{1}H NMR ($CDCl_3$, 300 MHz): δ 7.39–7.50 (m, 26H), 7.62–7.67 (m, 6H), 8.28 (d, ^3J = 7.8 Hz, 2H). ^{19}F NMR ($CDCl_3$, 470 MHz): δ – 62.64 (s).

Bis(triphenylphosphine)iminium pentafluorobenzoate (3.1, [PPN][OBzF_5], CTC-4-163) NaOH (190 mg, 4.7 mmol) and pentafluorobenzoic acid (1.0 g, 4.7 mmol) were added to a 50 mL round-bottomed flask charged with a Teflon stir bar. Distilled H_2O (20 mL) was added to the reaction mixture and it was stirred until all was dissolved. The solution was added to a 250 mL separatory funnel along with [PPN]Cl (400 mg, 0.7 mmol) and methylene chloride (40 mL), and the mixture was shaken vigorously for 10 min. The organic layer was collected and dried by rotary

evaporation to yield crude [PPN][$OBzF_5$] in quantitative yield. Precipitation from dry methylene chloride and diethyl ether under N_2 at –20 ºC afforded a white powder (350 mg, 67%). ^{1}H NMR ($CDCl_3$, 500 MHz): δ 7.39–7.46 (m, 24H), 7.60–7.63 (m, 6H). $^{13}C\{^1H\}$ NMR ($CDCl_3$, 125 MHz): δ 116.93, 126.91 (dd, $^1J_{P-C}$ = 108.0 Hz, $^3J_{P-C}$ = 1.5 Hz), 129.55 (m), 132.02 (m), 133.88, 137.07 (d of m, $^1J_{F-C}$ = 255.5 Hz), 139.92 (d of m, $^1J_{F-C}$ = 250.3 Hz), 143.24 (d of m, $^1J_{F-C}$ = 247.3 Hz), 161.21. ^{19}F NMR ($CDCl_3$, 470 MHz): δ –164.64 (m), -159.92 (broad s), –142.52 (m). Anal. Calcd for $C_{43}H_{30}F_5NO_2P_2$: C, 68.89; H, 4.03; N, 1.87. Found: C, 69.07; H, 3.95; N, 1.83.

Bis(triphenylphosphine)iminium tetraphenylborate (3.10, [PPN][BPh_4], CTC-4-181). 3.10 was prepared according to the procedure for [PPN][$OBzF_5$], but using sodium tetraphenylborate in place of benzoic acid and NaOH. Precipitation from dry methylene chloride and diethyl ether under N_2 afforded white crystals which were in accordance with previously reported characterization.[33, 34] ^{1}H NMR (CD_2Cl_2, 500 MHz): δ 6.84 (t, ^3J = 7.5 Hz, 4H), 6.99 (t, ^3J = 7.5 Hz, 8H), 7.29-7.32 (m, 24H), 7.61-7.64 (m, 6H).

3.11 References

(1) Qin, Z.; Thomas, C. M.; Lee, S.; Coates, G. W. *Angew. Chem. Int. Ed.* **2003**, *42*, 5484-5487.

(2) Darensbourg, D. J.; Yarbrough, J. C.; Ortiz, C.; Fang, C. C. *J. Am. Chem. Soc.* **2003**, *125*, 7586-7591.

(3) Allen, S. D.; Moore, D. R.; Lobkovsky, E. B.; Coates, G. W. *J. Am. Chem. Soc.* **2002**, *124*, 14284-14285.

(4) Eberhardt, R.; Allmendinger, M.; Rieger, B. *Macromol. Rapid Commun.* **2003**, *24*, 194-196.

(5) Darensbourg, D. J.; Yarbrough, J. C. *J. Am. Chem. Soc.* **2002**, *124*, 6335-6342.

(6) Darensbourg, D. J.; Phelps, A. L. *Inorg. Chem.* **2005**, *44*, 4622-4629.

(7) Darensbourg, D. J.; Mackiewicz, R. M.; Rodgers, J. L.; Phelps, A. L. *Inorg. Chem.* **2004**, *43*, 1831-1833.

(8) Darensbourg, D. J.; Mackiewicz, R. M.; Rodgers, J. L.; Phelps, A. L. **2004**, *43*, 1831-1833.

(9) Darensbourg, D. J.; Billodeaux, D. R. *Inorg. Chem.* **2005**, *44*, 1433-1442.

(10) Aida, T.; Ishikawa, M.; Inoue, S. *Macromolecules* **1986**, *19*, 8-13.

(11) Aida, T.; Inoue, S. *Acc. Chem. Res.* **1996**, *29*, 39-48.

(12) Lu, X. B.; Wang, Y. *Angew. Chem. Int. Ed.* **2004**, *43*, 3574-3577.

(13) Darensbourg, D. J.; Mackiewicz, R. M. *J. Am. Chem. Soc.* **2005**, *127*, 14026-14038.

(14) Darensbourg, D. J.; Mackiewicz, R. M.; Billodeaux, D. R. *Organometallics* **2005**, *24*, 144-148.

(15) Darensbourg, D. J.; Mackiewicz, R. M.; Phelps, A. L.; Billodeaux, D. R. *Acc. Chem. Res.* **2004**, *37*, 836-844.

(16) Sugimoto, H.; Inoue, S. *J. Polym. Sci. Polym. Chem.* **2004**, *42*, 5561-5573.

(17) Sugimoto, H.; Ohtsuka, H.; Inoue, S. *J. Polym. Sci. Polym. Chem.* **2005**, *43*, 4172-4186.

(18) Aida, T.; Inoue, S. *J. Am. Chem. Soc.* **1985**, *107*, 1358-1365.

(19) Aida, T.; Sanuki, K.; Inoue, S. *Macromolecules* **1985**, *18*, 1049-1055.

(20) Lu, X. B.; Liang, B.; Zhang, Y. J.; Tian, Y. Z.; Wang, Y. M.; Bai, C. X.; Wang, H.; Zhang, R. *J. Am. Chem. Soc.* **2004**, *126*, 3732-3733.

(21) Following our work, Lu and coworkers published similar studies concerning (salen)CoX catalyzed PO/CO_2 copolymerization: Lu, X. B.; Lei, S.; Wang, Y. M.; Zhang, R.; Zhang, Y. J.; Peng, X. J.; Zhang, Z. C.; Li, B. *J. Am. Chem. Soc.* **2006**, *128*, 1664 - 1674.

(22) Paddock, R. L.; Nguyen, S. T. *Macromolecules* **2005**, *38*, 6251-6253.

(23) Darensbourg, D. J.; Mackiewicz, R. M.; Rodgers, J. L.; Fang, C. C.; Billodeaux, D. R.; Reibenspies, J. H. *Inorg. Chem.* **2004**, *43*, 6024-6034.

(24) Aida, T.; Ishikawa, M.; Inoue, S. *Macromolecules* **1986**, *19*, 8-13.

(25) Martinsen, A.; Songstad, J. *Acta Chem. Scand. A* **1977**, *31*, 645-650.

(26) Inoue, S. *J. Polym. Sci. Polym. Chem.* **2000**, *38*, 2861-2871.

(27) Aida, T.; Maekawa, Y.; Asano, S.; Inoue, S. *Macromolecules* **1988**, *21*, 1195-1202.

(28) Aida, T.; Inoue, S. *J. Am. Chem. Soc.* **1983**, *105*, 1304-1309.

(29) Schaus, S. E.; Brandes, B. D.; Larrow, J. F.; Tokunaga, M.; Hansen, K. B.; Gould, A. E.; Furrow, M. E.; Jacobsen, E. N. *J. Am. Chem. Soc.* **2002**, *124*, 1307-1315.

(30) Chisholm, M. H.; Navarro-Llobet, D.; Zhou, Z. P. *Macromolecules* **2002**, *35*, 6494-6504.

(31) Lacroix, P. G.; Malfant, I.; Benard, S.; Yu, P.; Riviere, E.; Nakatani, K. *Chem. Mater.* **2001**, *13*, 441-448.

(32) Eda, M.; Kurth, M. J.; Nantz, M. H. *J. Org. Chem.* **2000**, *65*, 5131-5135.

(33) Reibenspies, J. H. *Z. Kristallogr.* **1994**, *209*, 620-621.

(34) Prakash, H.; Sisler, H. H. *Inorg. Chem.* **1968**, *7*, 2200-2203.